Multisensory Models for Human Spatial Orientation Including Threshold Effects

by

Raghav Harini Venkatesan

Submitted to the Department of Aeronautics and Astronautics
in partial fulfillment of the requirements for the degree of

Master of Science in Aeronautics and Astronautics

at the

MASSACHUSETTS INSTITUTE OF TECHNOLOGY

May 2010

Author……
Department of Aeronautics and Astronautics
May 25, 2010

Certified by……
Dr. Charles M. Oman
Senior Lecturer and Senior Research Engineer
Thesis Supervisor

Accepted by……...
Prof. Eytan H. Modiano
Associate Professor of Aeronautics and Astronautics
Chair, Committee on Graduate Students

MULTISENSORY MODELS FOR HUMAN SPATIAL ORIENTATION INCLUDING THRESHOLD EFFECTS

by Raghav Harini Venkatesan

Submitted to the Department of Aeronautics and Astronautics
on May 26, 2010 in Partial Fulfillment of the Requirements for the Degree of
Master of Science in Aeronautics and Astronautics

ABSTRACT: *E-Observer*, a stand-alone executable version of the *Observer* model developed by Newman and Oman (2009), was developed. The complicated structure of the *Observer* model and its parameters made this conversion challenging. The resulting Windows PC executable uses a publically available library (MATLAB component runtime v7.10). *E-Observer* parameters are limited to the preset choices in *Observer*. A hypothetical example of the use of *E-Observer* to analyze an aircraft accident radar trajectory data is discussed.

Like many other dynamic models for human spatial orientation, *Observer* does not incorporate perception thresholds, which limits its use to relatively large stimuli and hence cannot be used for investigation of certain accidents and flight simulator design, which involve sub-threshold motions. The literature on motion thresholds is reviewed which suggests that vestibular perception thresholds are not mechanical thresholds, but are due to signal-in-noise phenomenon.

As a first step towards incorporating thresholds in *Observer*, modeling yaw perception thresholds was attempted and two detection models are proposed – a Matched Filter model and a Two-Threshold model. The Matched Filter detector model matches the noisy perception with a noise-free stimulus template and evaluates how much they correlate. Based on the correlation, the model finally decides if the signal is present or not. However, this model applies only in cases where the subject is in an experiment, and knows the expected stimulus waveform. Grabherr et al (2008) proposed a high pass filter model for direction recognition thresholds based on their recognition data. This thesis explores an alternative modeling approach assuming that the CNS samples the angular velocity estimate and its derivative, and applies thresholds to both. Whether the motion stimulus is detected or not depends on how many of these samples cross the threshold level. The performance of both models was compared against the Grabherr et. al. data It was found that both models are able to approximate the 79.4% detection criterion for thresholds determined in Grabherr's study. However, the two threshold model does not assume that the subject knows the stimulus waveform. Supported by Project SA1302 by the National Space Biomedical Research Institute through NASA NCC 9-58.

Thesis Supervisor: Charles M. Oman, Ph. D.

Title: Senior Lecturer and Senior Research Engineer

ACKNOWLEDGEMENTS

I would like to thank Dr. Charles Oman for being my thesis advisor and providing me with the opportunity to work and research in the Man Vehicle Laboratory. I would also like to thank him for being very understanding in my tough times and also teaching how to approach research in general. The interesting discussions that we have had over the past few months were monumental to the development of the ideas in this thesis.

I would also like to thank Dr. Dan Merfeld and Dr. Larry Young for contributing their ideas.

Thank you to my parents Harini and Venkatesan, my fiancée Preethi, my friends Vinay, Raghu and others who have supported me mentally during these two years of study at MIT.

I would finally like to thank the National Space Biomedical Research Institute who supported this project (Project SA1302 R. Small, PI) through NASA NCC 9-58.

CONTENTS

CHAPTER 1: INTRODUCTION

A multisensory *Observer* model for human spatial orientation perception was developed by Newman (2009) for spatial orientation and eye movements, extending a previous vestibular-only model proposed by Merfeld and colleagues (1993, 2002). This model was ultimately to be included in Alion's Spatial Disorientation Analysis Tool (SDAT) and could also potentially be used by other external applications in the future. *Observer* runs in Matlab/Simulink. Hence it was desired to convert the Matlab version into a stand-alone executable version, E-Observer (executable Observer) that could be linked to SDAT, and that did not require an expensive MATLAB/Simulink license to run, only a publically available MATLAB component runtime library. Developing this stand alone executable was not a straightforward task, due to the structure of the *Observer* model, its parameters and GUI. Chapter 2 reviews the details of the *E-Observer* model development, defines inputs and outputs and parameter constraints. It also discusses the issues involved in the use of radar data to reconstruct aircraft trajectories as input to *E-Observer* in order to model spatial disorientation during aircraft accidents.

Like other models for human dynamic spatial orientation (as reviewed by Newman, 2009) *Observer* model does not incorporate thresholds for motion perception. Therefore, the model cannot be applied to flight simulator washout design and aircraft accidents that involve sub-threshold motions. For example, many common aeronautical spatial disorientation illusions, such as the "leans" involve sub-threshold motions. Flight simulator motions have to be washed out to limit cab displacements and this motion washout should be done at sub-threshold level to prevent false sensations. Also, sustained linear accelerations are simulated by tilting the cab with respect to gravity, and this should be done at sub-threshold levels to avoid the subject from knowing that he is being tilted and not accelerated. Because *Observer* is intended for these applications, it is important to incorporate thresholds into the *Observer* model.

Understanding human perceptual thresholds for rotation and translation is also important in several other contexts:

1) Perception of motion causes dizziness, giddiness, vertigo and motion sickness, which affect the well-being of an individual

2) Humans can assess vibration in vehicles and buildings only if the vibration is above the perceptual threshold.

3) Threshold testing may be a useful method of detecting vestibular disease in clinical settings.

In everyday life, perception of motion is not solely based on the vestibular organs. Visual auditory, proprioceptive and somatic cues also contribute to the perception of motion and also help in overcoming the limitation of the vestibular apparatus in sensing motion. The vestibular, visual, auditory, proprioceptive and somatic cues work in conjunction and in some situations improve the fidelity of motion perception. However, in case of motion in the dark or in environments which provide weak visual and auditory cues, perception of motion is primarily based on the vestibular organs as they are an order of magnitude more sensitive than proprioceptive and somatic senses (Mah et. al., 1989). Typically the lowest threshold values for angular and linear self motion perception are obtained from subjects studied in the dark.

It is to be noted that thresholds in motion perception are due to uncertainty in perception. This uncertainty in perceptions is in turn because of noise in vestibular afferents. The noise in vestibular afferents is assumed to propagate through CNS centers that estimate head orientation and finally manifests as noise in orientation perception.

In this thesis, two models for thresholds based on the perceptual noise in signal concept are proposed – a Matched-Filter Model and a Two-Threshold Model. The matched-filter model is an attempt to model yaw thresholds for single cycle sinusoidal acceleration stimuli from a recognition threshold experiment recently conducted by Grabherr et. al. (2008). In this experiment, the subject knew the frequency and waveform of the stimulus. The two-threshold model is however a more generic model and is not restricted to detection of only sinusoidal stimuli. The two-threshold model is based on an interesting trend observed from the yaw threshold data reported by Grabherr et. al. (2008). The two-threshold model can potentially be applied to model motion detection during the course of the stimulus, which the matched-filter model cannot. Suggestions for future validation experiments are made.

This thesis however does not apply any of the developed threshold models to *Observer*. This is because noise propagation in *Observer* has not been modeled yet, and hence the noise in perception at the output of *Observer* is not completely known. While modeling noise propagation in *Observer*, different noise sources should be used for each of the graviceptors. This is because the thresholds for x (naso-occipital) and y (interaural) axes are lower than that of the z-axis (dorsoventral), which suggests that noise in z-graviceptor could be higher than that in the x and y graviceptors. Similary, different noise sources should be used for each of the Semicircular canals. This is because yaw thresholds (about z-axis) are lower than roll (about x-axis) and pitch (about y-axis) thresholds, which

suggest that noise in roll and pitch could be higher than that in yaw. Also, it can be expected that the nonlinear dynamics of *Observer* might distort the Gaussian nature of the afferent noise by the time it percolates to the perceptions in the output. Therefore, the noise in perceptions may not be Gaussian, as assumed by the threshold models developed in the thesis.

Although the noise in perceptions may be non-Gaussian, it might still be possible to use the threshold models developed in this thesis, if it is in some way "equivalent" to the Gaussian noises assumed.

The final chapters discuss the simulation results from the two threshold models and suggest experiments to test the two-threshold model hypothesis.

CHAPTER 2: *E-OBSERVER* DEVELOPMENT AND RADAR DATA ANALYSIS

The *Observer* model was developed by Newman and Oman at MIT as an extension of the Merfeld et. al. (1993 & 2002) mathematical model for human dynamic spatial orientation, adding static and dynamic visual cues. *Observer* was originally developed in MATLAB/ Simulink matrix manipulation scripting language (Mathworks, Inc.), also utilizing its ordinary differential equation solvers and event-driven GUI capabilities. It was developed on the Windows, but runs on any MATLAB/Simulink compatible platform. However, a second goal was to link *Observer's* orientation predictions to Alion's Spatial Disorientation Analysis Tool (SDAT), a code which detects and classifies orientation illusions, and which is written in Alion's event simulation language, Micro Saint Sharp. Hence a stand-alone Windows version of *Observer* (*E-Observer*) was needed that could be run without the need for a relatively expensive MATLAB/Simulink license, and which could be called by SDAT. MATLAB/ Simulink R2009a was used in the making of *E-Observer*.

The initial challenge in making an executable version of *Observer* was in figuring out a way to convert a Simulink model into a stand-alone executable. Our original plan was to recode *Observer* Simulink blocks in native MATLAB, and then simply use the MATLAB compiler to create a stand-alone executable version. But this approach had its challenges, as some of the Simulink sub-system blocks inside *Observer* like the quaternion integrator have non-linear dynamics and cascading dynamic systems using MATLAB code is a difficult. The amount of code greatly increases and the program is inefficient. In fact, with some constraints (discussed below) most Simulink models can be converted to stand-alone Windows executables using a MATLAB Real-Time Workshop toolbox, a separately licensed development tool. The only constraint is that a library of Windows PC MATLAB routines, MATLAB component runtime v7.10, must be installed on the target machine. (This library is available from the Mathworks at no cost to users.). The resulting executable matches the functional behavior of most Simulink simulations to a high degree of accuracy.

One of the features of the *Observer* model is that it has a Graphical User Interface (GUI) for selecting input files, setting model parameters and visualizing simulation results, as shown in Fig. 2.1.

It is possible to also convert a GUI into an executable using MATLAB Compiler, but the *Observer* GUI had calls to the *Observer* Simulink model during runtime. Since the *Observer* model itself was going to be converted into an executable, and given the

structural complexity of the *Observer* model and its executable (as will be explained later), it was not a straightforward task to create a GUI executable using MATLAB Compiler, that would call *E-Observer* in turn.

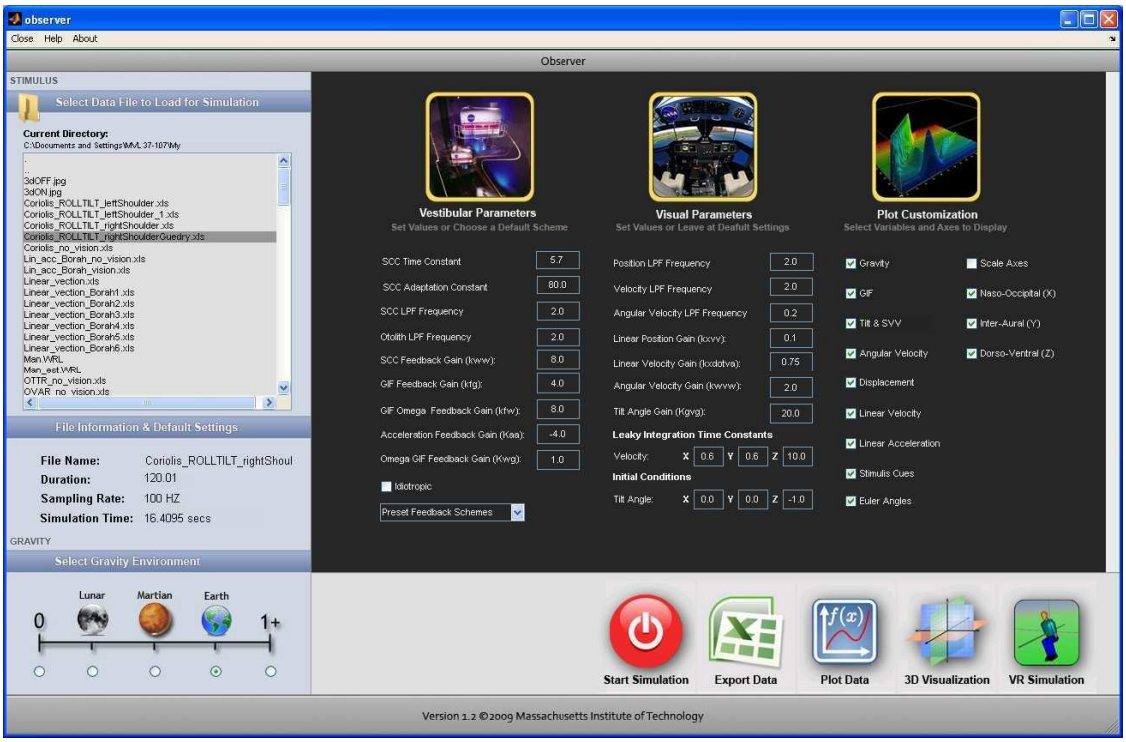

Fig. 2.1 – GUI of *Observer* Model designed by Newman and Oman

Also, applications like the SDAT have their own GUI and when used with SDAT, *E-Observer* would just be the engine that would compute spatial orientation estimates. So it was decided to remove the GUI interface for *E-Observer*. This required that the input files and parameters to *E-Observer* be passed explicitly from the external application. Also, another program had to be created that would fetch *E-Observer*'s output and allow the user to visualize of the results. The following sections are programmers notes detailing the development, the rationale for the approach taken and for some of the compromises inevitably made, and some notes on how to change E-Observer internal parameters. In the following sections it is assumed that the reader has general familiarity with MATLAB, Simulink, and Newman's 2009 Observer model. Users not interested in these details can skip directly to Section 2.3.

2.1 INPUTS TO *E-OBSERVER*

The *Observer* model reads an excel file (chosen from the list in the left of the GUI in Fig. 2.1) containing time series data for various variables listed in Pg. 55 & Pg. 56 of

Newman's thesis (2009) as input and writes the data into its workspace. The visual and vestibular parameters (the first two columns in the GUI) are also transferred to its workspace.

The *Observer* Simulink model has an input structure as shown in Fig. 2.2. The rectangular blocks on the left are 'From Workspace' blocks and they get the excel-file data stored in the workspace into the model. The other blocks read their respective parameters directly from the workspace. Therefore, with this structure, the visual and vestibular parameters and the input data all become parameters for various blocks in the *Observer* model. As explained later, this feature of *Observer* structure had disadvantages.

2.2 CONVERTING *OBSERVER* INTO *E-OBSERVER*

While compiling the *Observer* model with Real-Time Workshop into a stand-alone executable, the 'System target file' was chosen to be **rsim.tlc** and the solver was set to fixed-type ode5 (Dormand-Prince) solver. This was done because executables of Simulink models cannot be created using a variable-step solver. The values for the 'System target file' and solver can be set from the 'Configuration Parameters' for the *Observer* model.

Before a Simulink model can be compiled into an executable, all the parameters for the model must be set. Therefore, to set the parameter values for *E-Observer*, some input file and the default set of visual and vestibular parameters were used.

The executable was then be created by using the 'Build' command from the 'Real Time Workshop' menu under 'Configuration Parameters'. However, the *Observer* model has a lot of parameters and the GUI allows users to change these parameter values and input excel file in the MATLAB version. However, *E-Observer* created as described above did not provide any capability to tune its parameters.

It was found that the parameters of the compiled model could be changed by altering the parameter file *parameter_struct.mat* for the *Observer* model, created by the following MATLAB commands:

```
parameter_struct = rsimgetrtp('observerModel.mdl');
save parameter_struct.mat parameter_struct
```

where, the file *observerModel.mdl* is the Simulink version of the *Observer* model. The file *parameter_struct.mat* contains a structure called *parameter_struct* that stores details about the model's properties. The structure *parameter_struct* in turn contains a variable called *modelChecksum* and another structure called *parameters* inside it.

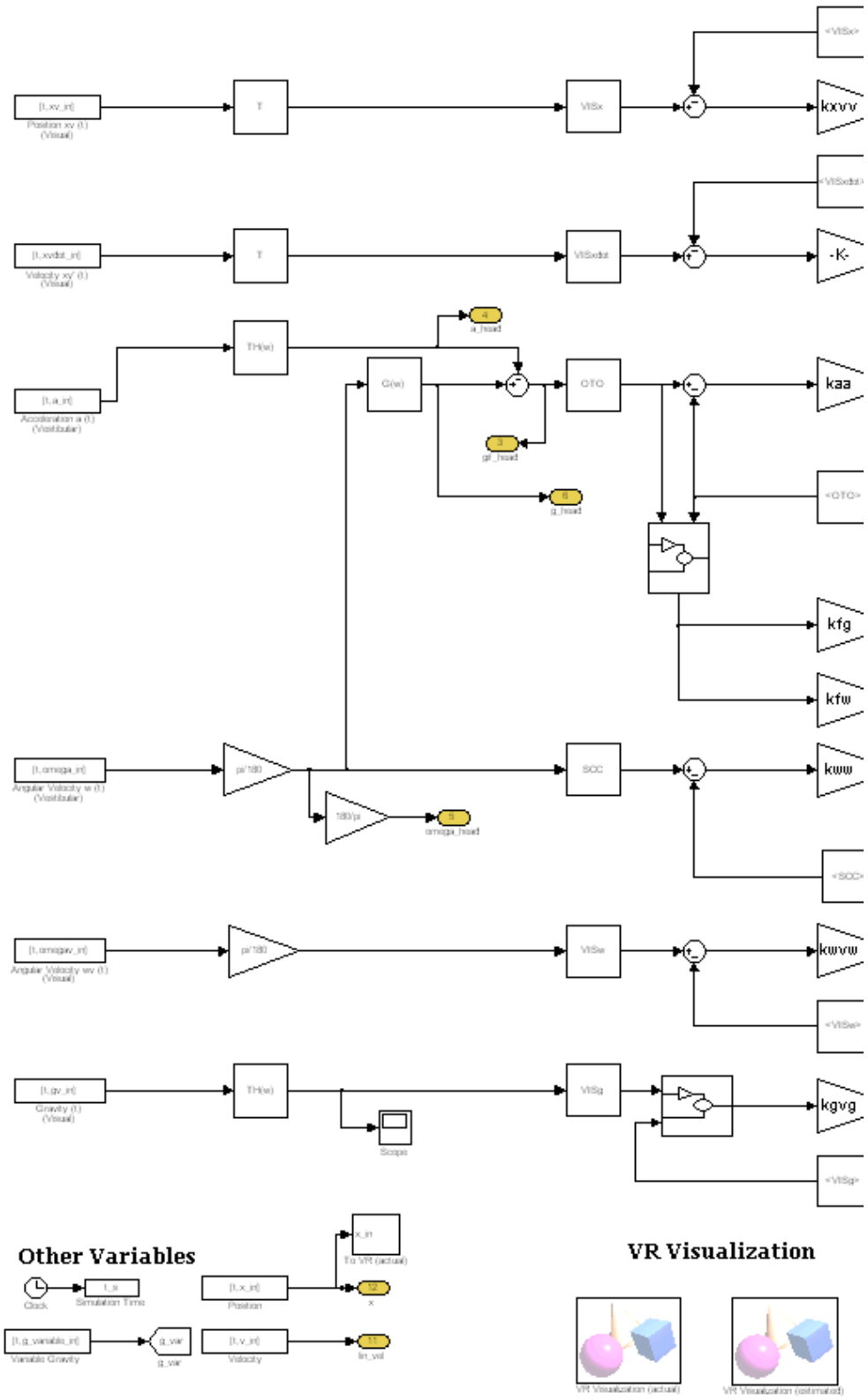

Fig. 2.2 Input structure for *Observer*

The variable *modelChecksum*, generated by Real-Time Workshop for a Simulink model has a one-to-one relation with the executable that is created for the same model. In other words, if *Observer* has to be converted into an executable with a provision for tuning its parameters, it should be compiled and the parameter file *parameter_struct.mat* should be generated together without making any changes to the model between the two steps. If the model is changed between these two steps in any way, the *modelChecksum* in *E-Observer* and *parameter_struct* would not tally and this would prevent *E-Observer*'s parameters from being tuned.

The data structure *parameters* inside *parameter_struct* has five more structures within it, of which, only the first structure is of interest. The remaining four structures are generated due to Virtual Reality blocks used in the *Observer* Simulink model.

Within the first structure, i.e. *parameter_struct.parameters(1,1)*, there is a variable called *values,* which stores the values for all the parameters of the *Observer* model. Because of the structure of *Observer* as described in Section 2.1, the variable *values* also had time series data inside it. Now, if input files of different time lengths are used, they would affect the length of this variable *values*. When the *Observer* model was first converted to an executable version, *values* was sized in many thousands, and figuring out the locations of parameters inside it was an impractical task. Also, the length of *values* had to be changed externally depending on the time length of the input file..

It was then found that this problem could be eliminated if the input data are passed though input files instead of passing them as parameters as in the original *Observer* Simulink Model. So it was decided to change *Observer*'s input structure by using a 'From File' block, containing the excel file data as shown in Fig. 2.3. This approach made sure that the input data are never passed as parameters to the Simulink model. Therefore, when *parameter_struct.mat* was created for this model, the number of parameters in it was a constant value. As mentioned earlier, these parameters are stored in the variable *parameter_struct.parameters(1,1).values*. This constant number of parameters was found to be 327.

Next, to determine what parameters were stored in the various cells, several trials were conducted by changing the parameter values one by one and monitoring which cell in the *values* changes. Some of the cells changed in a complex way when values are changed, whereas others straight forward. The cells that changed in a complex way had cross-coupling between them. How the various parameters of *Observer*'s GUI affect the various cells of *values* is tabulated in Table 2.1.

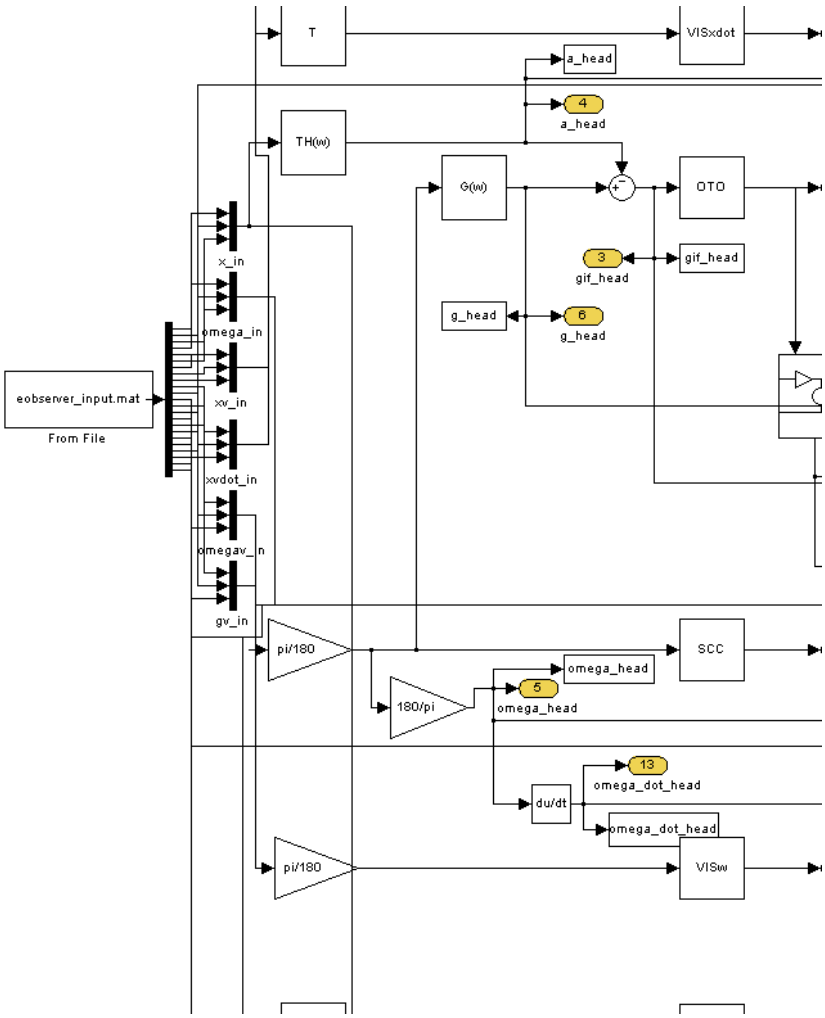

Fig. 2.3 – Modified *Observer* input structure using a 'From File' block for making *E-Observer*

To understand Table 2.1, the following should be noted:

1) The poles of the semi-circular canal are **-1/tau_scc, -1/tau_a, 2π*f_scc**
where *tau_scc* is the Semicircular Canal (SCC) time constant, *tau_a* is the SCC adaptation constant, and *f_scc* is the SCC low pass filter frequency.

There are no zeros in the transfer function for the SCC. The gain for the SCC is denoted by ***gain***.

Parameter	Affected locations inside *values*	Relationship
SCC time constant SCC adaptation constant SCC lpf frequency	57, 66, 75	min(poles)
	59, 68, 77, 84, 89, 94	Sum of the other 2 poles than the minimum
	60, 69, 78, 85, 90, 95	Negative square root of of product of the other 2 poles than the minimum
	61, 70, 79, 86, 91, 96	Positive square root product of the other 2 poles than the minimum
	64, 73, 82	gain*(Sum of the other 2 poles than the minimum)
	65, 74, 83	Gain*Negative square root of product of other 2 poles than the minimum
Otolith lpf frequency	1, 2, 3, 4, 5, 6, 7, 8, 9, 10, 11, 12, 163, 164, 165, 166, 174, 175, 176, 177, 185, 186, 187, 188	
Scc feedback gain kww Omega gif feedback gain, kwg	99, 100, 101	kww
	291, 292, 293	1+1/(kww+2)
	294, 295, 296	1+1/kww
	297, 298, 299	(1+1/(kww+2))*kwg
	300, 301, 302	(1+1/kww)*kwg
Gif feedback gain, kfg	157, 158, 159	kfg
Gif omega feedback gain, kfw	54, 55, 56	kfw
Acceleration feedback gain, kaa	13, 14, 15	kaa
Linear position gain kxvv	306, 307, 308	kxvv
Linear velocity gain kxdotva	303, 304, 305	kxdotva
Angular Velocity gain kwvw	291, 292, 293, 297, 298, 299	1+1/(kwvw+2)
	309, 310, 311	kwvw
Tilt angle gain kgvg	288, 289, 290	kgvg

Table 2.1 – Table of the locations that are affected by *Observer*'s parameters and relations

This table above is provided so that it can be used if any parameter has to be tuned by any application that may use *E-Observer* in the future. For example, if an application wants to change the 'kxvv' for *E-Observer*, it would access the *parameter_struct.mat* file and change the 306, 307 and 308th cells of the variable *parameter_struct.parameters(1,1).values* to the new value. Similarly, if the value of 'kwvw' is to be changed, the expression in the third column '1+1/(kwvw+2)' has to be computed for the new 'kwvw' value and put in cells 291-293 & 297-299, and also the new 'kwvw' value has to be put in 309-311.

2.3 USING *E-OBSERVER* FOR PREDICTING SPATIAL ORIENTATION

For the *E-Observer* executables to run, MATLAB component runtime v7.10 has to be installed in the target machine. This freeware library is provided along with the executables described below.

E-Observer also requires an input file for e.g. *eobserver_input.mat* as shown in Fig. 2.3 to run. This file is a transformation of the input excel file used in *Observer* into a mat file. This mat file contains a variable which 24 rows of data corresponding to the 24 columns of the input excel file as described in Pg. 55 & Pg. 56 of Newman's thesis.

To display the predicted spatial orientation, another program is required that will read the output file generated by *EObserver* and plot the various variables of interest.

To achieve the above processes, and for using *E-Observer* to predict spatial orientation, the following programs were developed:

1) *eobserverInit.exe*, to generate the input file and the parameter file for *E-Observer*
2) *eobserverModel.exe* – also known as the *E-Observer*
3) *eobserverOutput.exe*, to generate the output file and graphically display the results

These executables are run from the windows command line. It was decided that the E-Observer user would be restricted to choosing one of the five parameter sets detailed in Newman's thesis and presented as options in *Observer*'s GUI:

1) haselwanter_2000_human
2) merfeld_1993_monkey
3) merfeld_2002_human
4) merfeld_2002_monkey
5) vingerhoets_2007_human

Therefore *eobserverInit.exe* takes the input excel file used in *Observer* and the vestibular parameter model as input and generates a mat file as output, which would in turn become *E-Observer*'s input. It also accesses the *parameter_struct.mat* file for *E-Observer* and changes the vestibular and visual parameters in their appropriate cell locations. For example, to generate a mat file *input1.mat* that contains the data of *Yaw_Borah.xls* and to have *E-Observer* simulated with the 'vingerhoet_2007_human' parameters, the following command would be issued at the command prompt:

```
eobserverInit Yaw_Borah.xls input1.mat vingerhoets_2007_human
```

Once the input mat file to *E-Observer* and the *parameter_struct.mat* file are ready, *eobserverModel.exe* is run using the following command from the command prompt:

```
eobserverModel -p parameter_struct.mat -f eobserver_input.mat=input1.mat -o
output1.mat
```

When the above command is used, the *E-Observer* executable *eobserverModel.exe* takes *parameter_struct.mat* as the parameter file, *input1.mat* as the input file and writes its output to *output1.mat* file. Because the input file to *E-Observer* was hard coded as *eobserver_input.mat* as shown in Fig. 2.3, to change it to *input1.mat*, the command "`-f eobserver_input.mat=input1.mat`" is used.
Now, to graphically display the output of *E-Observer*, the program *eobserverOutput.exe* is run using the following command from the command prompt:

```
eobserverOutput output1.xls output1.mat output
```

This program *eobserverOutput.exe* takes the output of *E-Observer*, *output1.mat* as input and writes the data in it into the excel file *output1.xls* in the worksheet *output.* It also displays the estimated spatial orientation in a bunch of plots. Unlike the original *Observer*, *E-Observer* does not have the capability of 3-D and Virtual Reality (VR) visualization.

2.4 AN EXAMPLE DEMONSTRATING THE USE OF *E-OBSERVER* TO PREDICT SPATIAL DISORIENTATION USING RADAR DATA

This example, assumes that the user is an NTSB investigator, analyzing an aircraft accident using a dataset from a precision approach radar (PAR), which contains the 3D position data of the aircraft. (The data used in this example is hypothetical, and doesn't include noise typically found in real data. In real world examples, radar noise must be smoothed. Also, often the available radar data is from slower ASR radars. Low radar update rates rates and noise typically limit the user's ability to accurately estimate true

aircraft angular and linear acceleration.) Radar data is in a world coordinate frame. The linear acceleration and angular velocities required by *E-Observer* must be transformed into the coordinate frame of the pilot's head. For this example it is assumed that perceived orientation is based on vestibular cues alone. However, if visual orientation data can be estimated, in could be included in the analysis, using the methods explained. . The purpose of the example is to illustrate the analysis of aircraft radar based 3D position data using *E-Observer* to predict spatial disorientation.

2.4.1 APPROACH RADAR DATA AND CHARACTERISTICS:

Airport Surveillance Radars (ASR) are one of the approach radars used in airports for aircraft surveillance. The scan rate for the radar is 12.5 rpm, which translates to 1 scan every 4.8 sec. Therefore the update rate for the radar is roughly 0.2 Hz. ASR-9 and ASR-11 radars are the most extensively used radars with ASR-11 being a low cost solution for aircraft surveillance at secondary airports. Secondary Surveillance Radars (SSR) used in airports have a faster scan rate at 15 rpm, which corresponds to one scan every 4 seconds. They also have a higher range (100 nautical miles), compared to ASR which have only a maximum range of 30 nautical miles. There are also Precision Approach Radars (PAR) used in capacity constrained airports which have a faster update rate than ASR/ SSR at 1 scan per second. However, their maximum range is just 20 nautical miles which is lesser than even ASR. There are also Air Route Surveillance Radars (ARSR) which are center based radars, and have a scan rate of 5 rpm. The example discussed here assumes the best update rate, as it simulates data from the PAR.

2.4.2 LIST OF REQUIRED FILES AND PROGRAMS FOR THIS EXAMPLE

1) An excel file containing 3D position data of the aircraft from the radar, *radar_data.xls*
2) A program (*generateObserverInput.exe*) that reads *radar_data.*xls and generates an excel file of derived variables (*flightvariables.xls*) and an excel file (*observerInput.xls*) that is an input for *eobserverInit.exe.*
3) *parameter_struct.mat*
4) *eobserverInit.exe*
5) *eobserverModel.exe*
6) *eobserverOutput.exe*

2.4.3 PREDICTING SPATIAL DISORIENTATION

A schematic describing the process to predict spatial disorientation is shown in Fig. 2.4.

The difficult step using *E-Observer* is organizing the radar data in *Observer*'s input format. Therefore, in the following sections, the procedure and specifications to build the input excel file *observerInput.xls* for accident investigation using *E-Observer* are described. The analysis process is detailed, although for brevity the results generated are not scientifically interpreted.

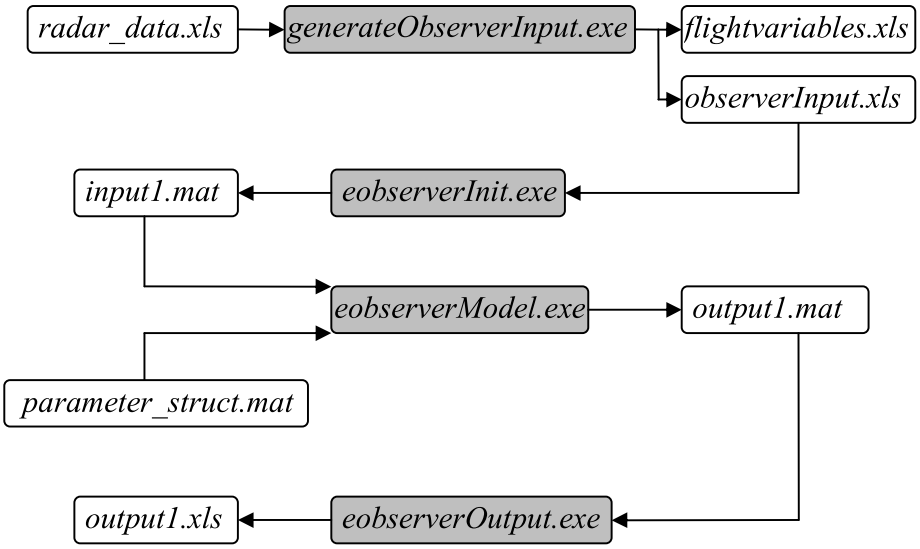

Fig. 2.4 – Schematic of the process to predict spatial disorientation

2.5 GENERATING THE INPUT FILE FOR OBSERVER FROM RADAR DATA

It is assumed that the following data is available in a data file *radar_data.xls* typically:

1) Lift coefficient data C_L as a function of the angle of attack α for the aircraft wing, used to estimate angle of attack.
2) Various constants of the aircraft and relations between various parameters
3) The actual radar data.

The hypothetical example described here assumes that data is available at 1 Hz which corresponds to that of a Precision Approach Radar (PAR). A snapshot of the data used for the example is shown below. The data contains the aircraft's East-West coordinate position, North-South coordinate position, altitude and messages from the radio transmission.

The program *generateObserverInput.exe* was designed to generate the input file for *eobserverInit.exe*. From the command line, this program was called by:

```
generateObserverInput radar_data.xls flightvariables.xls observerInput.xls off
```

The *generateObserverInput.exe* program takes four inputs. The first input is the excel file containing radar data. The second input (*flightvariables.xls* in this case), is the name of the excel file that is output containing the various variables of flight such as the roll rate, yaw rate, wind speed etc. using standard aerodynamic relations. The third input is the name of the excel file (*observerInput.xls* in this case) that will be generated as an input to *eobserverInit.exe*. The fourth input is a Boolean value *on* or *off* indicating whether vision is on or off. Since it is assumed that there is no visual input in this example, the fourth input is *off*.

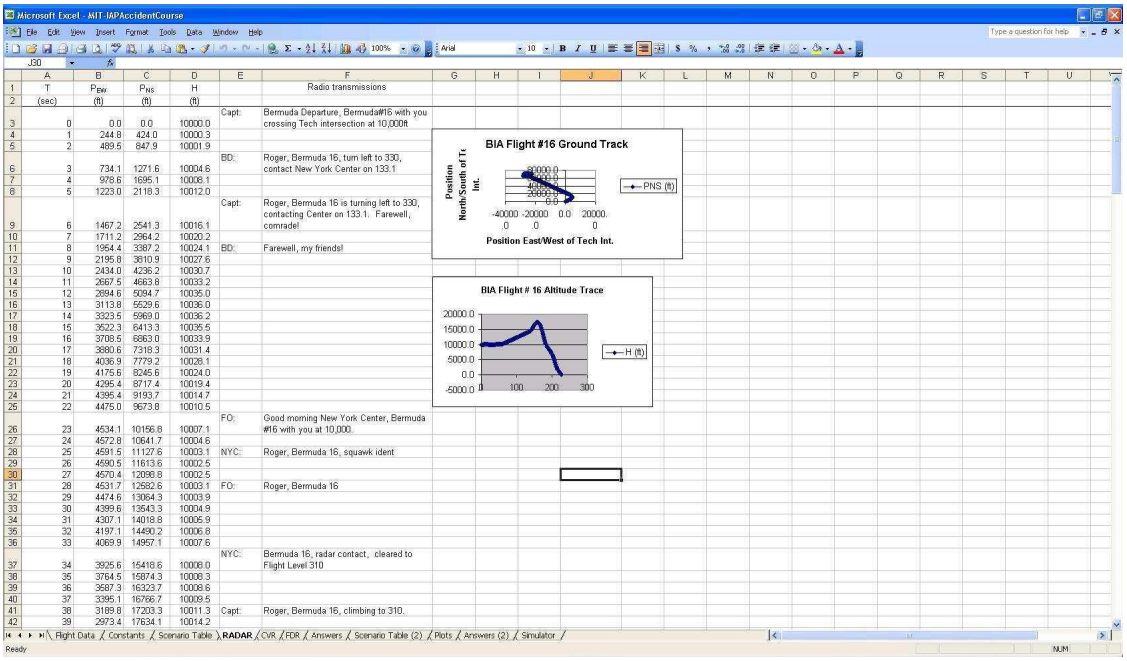

Fig. 2.5 – Snapshot of Radar data

The file *flightvariables*.xls is provided to allow the user to look up the various variable of flight if interested.

The angular velocities, linear velocities and position of the aircraft calculated from the radar data should go to the various columns of *observerInput.xls* according to the specifications in Newman's thesis for *Observer*.

2.5.1 WORLD AND HEAD COORDINATE FRAMES

The radar data are assumed to be in a world coordinate frame, and hence all the variables calculated from them like the velocities and angular velocities are also in the world coordinate frame. However *Observer* and *E-Observer* require that the angular velocities be in the pilot's head coordinate frame. Therefore, the angular velocities need to be transformed from the world to head coordinate frame. This transformation can be achieved through a quaternion implementation and the program *generateObserverInput.exe* was designed to do this operation.

2.5.2 VISUAL INPUT 'OFF'

If it is assumed that there is no visual input, then *observerInput.xls* work sheet should appear as in Fig. 2.6. The last four columns that correspond to visual switches for position, velocity, angular velocity and gravity are all '0' at all times. The positions and angular velocities calculated go to the vestibular part and are populated from columns B-G. Correspondingly, columns H-J and N-P are '0' as there are no visual positions and angular velocities. There visual velocities are the same as vestibular velocities and are populated in columns K-M. However, although these cells may be populated, they are overridden by the visual velocity switch in column V. If column V reads 0's, even if columns K-M are populated, they will not be used by *E-Observer*. Only if column V reads 1's, the values in columns K-M will be used. Therefore, column V is populated with 0's in this case.

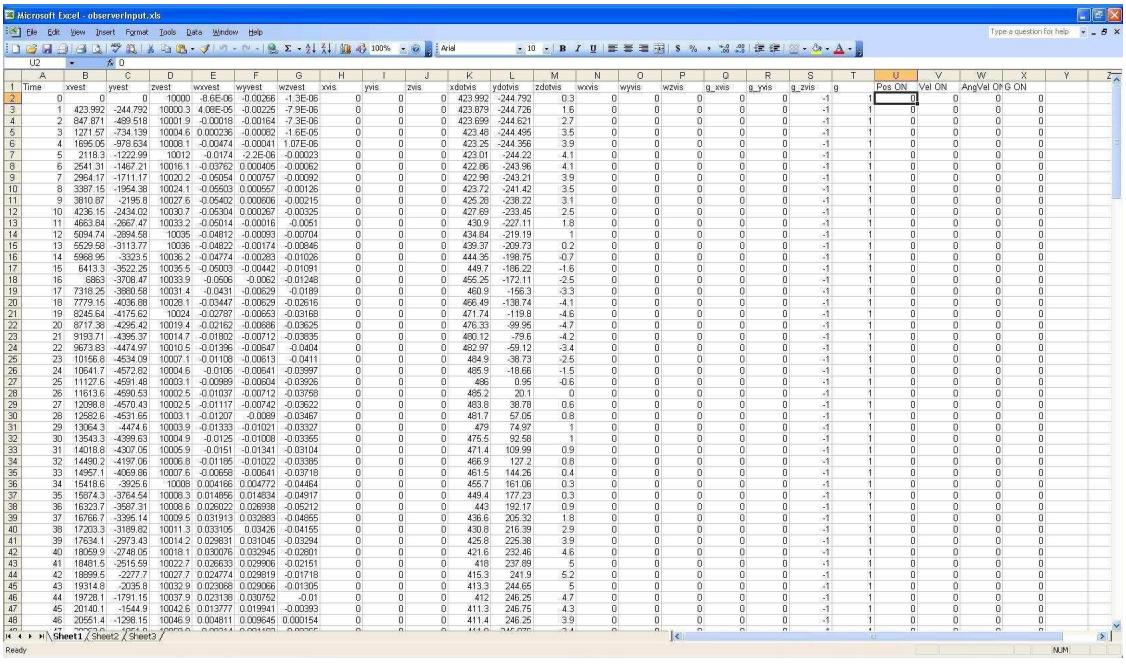

Fig. 2.6 – *observerInput.xls* file with visual input off

2.5.3 VISUAL INPUT 'ON'

When vision is 'on', two cases should be considered:

1) The pilot gets visual cues just from the cockpit. The input file for this case is shown in Fig. 2.7.
2) The pilot gets visual cues from the world outside – The input file for this case is shown in Fig. 2.8

When the visual cues are restricted to the cockpit, the pilot perceives 'down' along the perpendicular to the floor of the aircraft. According to Newman's specification for *Observer*, columns Q-S in *observerInput.xls* should be in world coordinates. But as the aircraft itself has a pitch angle, the world coordinates of perceived 'down' are $\sin\theta$ and $\cos\theta$, where θ is the pitch angle. There are no visual position, visual velocity and visual angular velocity cues, as the pilot does not see the outside, and hence all the corresponding switches in columns U-W are '0'. The only visual cue is gravity and hence column X is filled with 1's, as shown in Fig. 2.7.

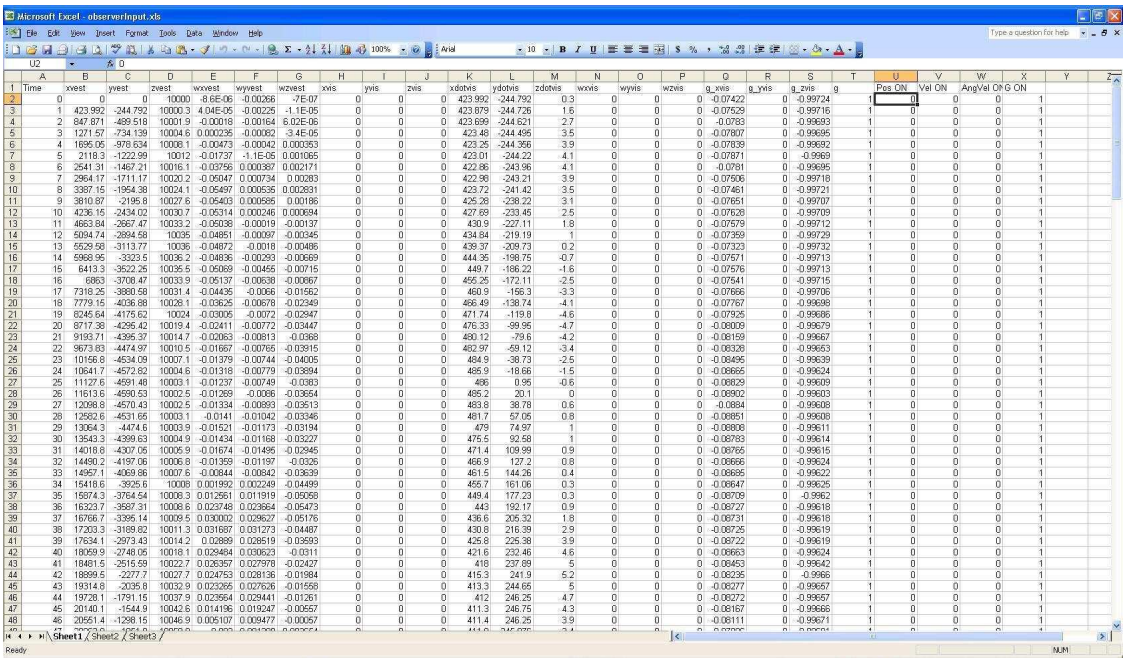

Fig. 2.7 – *observerInput.xls* file with visual input 'on' – cockpit view

However, when the pilot has full view of the outside world through the window, visual cues provide position, linear velocity, angular velocity and 'down' information, and agree with that of the vestibular sense. Therefore, columns B-D and H-J are the same, and columns E-G and N-P are the same. Also, all the visual switches, columns U-X are 'on' in this case. These are shown in Fig. 2.8

2.6 ESTIMATING SPATIAL ORIENTATION

Now, to estimate the spatial orientation and display the results for *observerInput.xls* using the Vingerhoets 2007 human model for vestibular parameters, the following commands are executed as explained in Section 2.3.

```
eobserverInit observerInput.xls input1.mat vingerhoets_2007_human

eobserverModel -p parameter_struct.mat -f eobserver_input.mat=input1.mat -o
output1.mat

eobserverOutput output1.xls output1.mat output
```

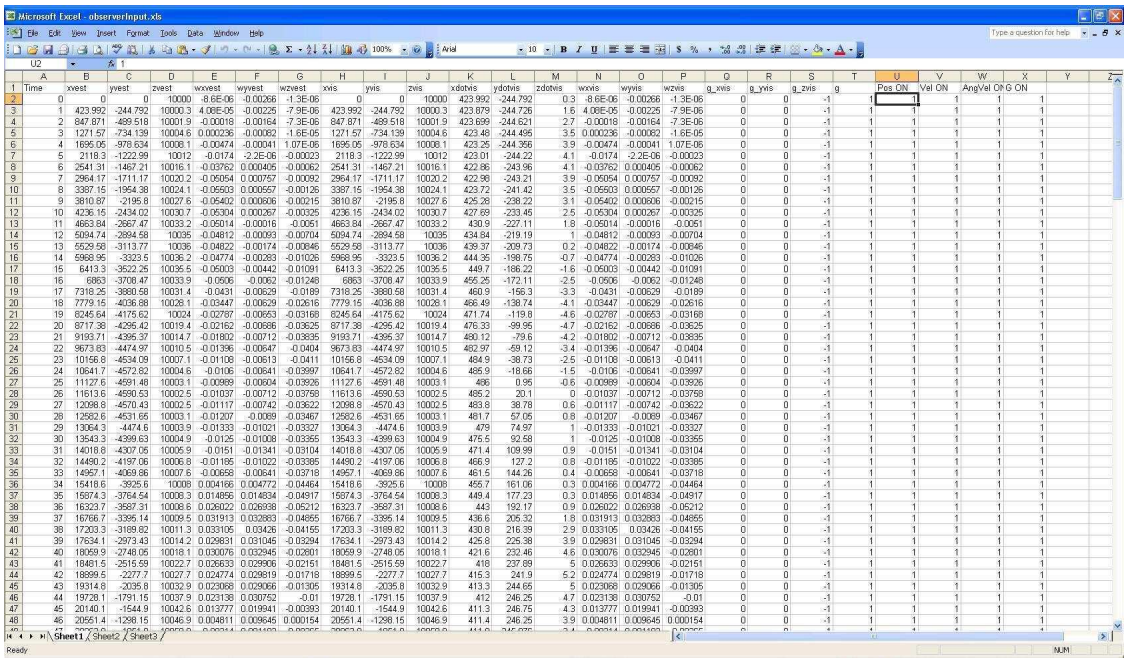

Fig. 2.8 – *observerInput.xls* file with visual input 'on' – full outside view

CHAPTER 3: BACKGROUND

Thresholds for motion perception are affected by various factors such as the profile of the stimulus, psychophysical method used to determine the thresholds, orientation with respect to gravity, and various other factors. [The following sections are adapted from a 2010 term paper prepared by the author for MIT course 16.430J Sensory Neural Systems].

3.1 EFFECT OF MOTION STIMULUS PROFILES

Motion perception thresholds depend on the type and axis of stimulation relative to the subject and to gravity. This is very evident from the literature, summarized in Table 3.1.

Author	**Type of Stimulus**	**Principal Axis**	**Initial conditions (if different from nominal)**	**Threshold Type**	**Threshold Values ($deg.s^{-1}$, $deg.s^{-2}$ or sec)**
Clark and Stewart (1962)	Constant acceleration	z-axis (dorsoventral)	-	Recognition	0.12-0.17 $deg.s^{-2}$
Clark and Stewart (1969)	Constant acceleration	z-axis (dorsoventral)	-	Recognition	0.05-2.20 $deg.s^{-2}$
Gundry (1978)	Constant acceleration with varying magnitudes from 0.01 to 8 $deg.s^{-2}$	x-axis (horizontal)	Subject upright	Recognition	0.2-20 sec
		x-axis (vertical)	Subject in supine position	Recognition	0.5-6 sec
		x-axis (horizontal)	Subject on his side	Recognition	0.5-40 sec
Benson et. al.(1989)	Single cycle sinusoidal acceleration stimulus of 3.3 sec duration	z-axis (dorsoventral)	-	Recognition	Mean: 1.58 $deg.s^{-1}$ SD: 2.3 $deg.s^{-1}$
		y-axis (interaural)			Mean: 2.07 $deg.s^{-}$

					[1] SD: 2.23 deg.s^{-1}
		x-axis (naso-occiptal)			Mean: 2.04 deg.s^{-1} [1] SD: 2.23 deg.s^{-1}
		z-axis (order effect)			Mean: 1.20 deg.s^{-1} [1] SD: 2.64 deg.s^{-1}
	Single cycle sinusoidal acceleration at 6 durations logarithmically disposed between 0.9 and 20 sec	z-axis (dorsoventral)	-	Recognition	9.3362 deg.s^{-1} to 0.9338 deg.s^{-1} as duration of the stimulus decreases
Grabherr et. al. (2008)	Single cycle sinusoidal acceleration at 7 frequencies of 0.05,0.1,0.2,0.5,1,2 and 5 Hz	z-axis (dorsoventral)	-	Recognition	Mean values of 2.84, 2.51, 1.66, 0.73, 0.64, 0.38 and 0.59 deg.s^{-1}

Table 3.1 – Angular motion thresholds from the literature

Table 3.1 contains data of angular motion perception thresholds for various stimulus profiles, orientations and perceptual modes in the literature. Principal axis is the axis about which angular motion stimulus is administered with respect to the subject. Thresholds are quantified in units of deg.s^{-1} for velocity thresholds (peak velocity attained for a sinusoidal acceleration stimulus), deg.s^{-2} for acceleration thresholds and sec for thresholds expressed in terms of latency for the corresponding acceleration stimulus profile. All the thresholds reported in the studies are 'recognition thresholds' – a term which will be explained later.

From Table 3.1, comparing the results of Clark and Stewart (1962&1969), Benson et. al. (1989) and Grabherr et. al. (2008) it is evident that for same axis of testing (dorso-ventral z-axis), threshold values for constant acceleration stimulus profiles are different from that of sinusoidal acceleration stimulus profiles, and are quantified in different units (deg.s^{-2}

for constant acceleration stimuli and deg.s^{-1} for the peak velocity in case of sinusoidal acceleration stimuli).

Author	Type of Stimulus	Principal Axis	Threshold Type	Threshold Values
Benson et. al. (1986)	Single cycle sinusoidal acceleration of duration 3 sec	x-axis (naso-occipital)	Recognition	Mean: 0.063m.s^{-2} SD: 0.13 m.s^{-2}
		y-axis (interaural)		Mean: 0.057 m.s^{-2} SD: 0.12 m.s^{-2}
		z-axis (dorsoventral)		Mean: 0.153 m.s^{-2} SD: 0.13 m.s^{-2}
	Single cycle sinusoidal acceleration of varying durations 0.98,1.93,3.84 and 6.84 sec i.e. 0.14 Hz to 1.02 Hz	x-axis(naso-occipital)		0.453, 0.662, 0.67 and 0.883 m.s^{-2} respectively
Mah et. al. (1989)	Sinusoidal acceleration stimuli of varying number cycles depending on the frequency – Frequency range: 0.2 Hz -3 Hz	-	Detection	0.002 – 0.004 milli-g's and varying as a function of frequency

Table 3.2 – Linear motion thresholds from the literature

Also, looking at results from Benson et. al (1989) and Grabherr et. al. (2008) in Table 3.1, and Benson et. al. (1986) in Table 3.2, it is evident that even within sinusoidal acceleration stimulus profiles, both angular and linear thresholds generally depend on the frequency of the stimulus. The trend is that threshold values increase as frequency decreases. (Note: Mah et. al (1989) found no dependence of linear motion thresholds on frequency. But at low frequencies, accelerations will be interpreted as tilt and hence the results from Mah et. al.'s study may be only valid for the frequencies they studied.) Understanding the dependence of motion thresholds on frequency of the stimulus is more

easily understood by reviewing how angular rotation thresholds have been modeled, historically:

3.1.1 HISTORY OF ANGULAR ROTATION THRESHOLD MODELING

Mulder (1908) experimentally found that for constant yaw acceleration stimuli less than 10 sec, the product of acceleration stimulus and the time upright subjects took to report motion was approximately a constant, thus suggesting an angular velocity threshold for the perception of brief yaw motions.

Groen and Jongkees (1948) explained Mulder's finding using the torsion pendulum model for Semicircular Canal cupula-endolymph mechanics. They noted that cupula displacement was proportional to head angular velocity for brief rotations, and proportional to head accelerations at low frequencies, and assumed that there was a threshold cupular displacement below which rotation wouldn't be felt.

However, physiological studies later by Goldberg and Fernandez (1971) showed no existence of mechanical thresholds but did quantify the noise in the vestibular afferent signals. This suggested that the threshold process was not mechanical, but a perhaps phenomenon that arose due the presence of noise in the sensory signal. Therefore, when modeling rotation perceptions, Ormsby & Young (1977) and Sivan et. al. (1982) proposed that an optimal estimator separated the rotational signals from afferent noise. Subsequently, Borah et. al. (1988) used a multiple sensor Kalman filter to model perceptions, where sensor noise ultimately produced noise in estimates of angular and linear velocity and tilt. This approach suggested that **perceptual thresholds are due to noise in central nervous system estimates of orientation and motion** and not in the afferent signals themselves, a notion which is now widely accepted.

This model for thresholds is also supported by the fact that frequency dependence of yaw thresholds from a more recent study by Grabherr et. al. (2008) could not be explained by the torsion pendulum model for the semicircular canals or the velocity storage model (Fig. 3.1). (Velocity storage is the mechanism by which the perception of angular motion outlasts the angular velocity signal from the Semicircular Canal afferents.)

Hence it can be argued that currently the most generally accepted approach to modelling human thresholds is to view it a "signal in noisy perceptions" problem.

3.2 EFFECT OF PSYCHOPHYSICAL METHODS

While testing vestibular thresholds, scientists in the past have always asked their subjects to report only when they sensed the direction of motion, and not just when they detected motion. One difference is the study by Mah et. al. (1989), where they employed a 2-interval forced choice procedure, with one interval containing the stimulus and the other containing no stimulus. They assigned ratings to how much information the subjects were able to get out of the experiment – different ratings were assigned to the subjects guessing compared to subjects being able to tell the direction(s) of motion.

It is not practical to present a large number of stimuli in vestibular testing unlike auditory testing, as motion perception experiments are time consuming and the subjects frequently get fatigued or become motion sick. When low frequency stimuli (long duration) are used for motion testing in the dark, it also becomes difficult to prevent the subjects from falling asleep. Therefore, vestibular scientists always work towards reducing the number of motion stimuli presented to reach thresholds. Scientists have used various psychophysical methods such as double-staircase method (Clark & Stewart, 1969), method-of-limits (Gundry, 1978), Hybrid Parameter Estimation by Sequential Testing (PEST) (Benson et. al. 1986) and 3-down 1-up staircase method (Grabherr et. al., 2008) to determine motion thresholds.

The method-of-limits procedure used by Gundry (1978) suffers from the errors of habituation and anticipation. In this procedure, stimuli are either presented in an ascending (stimuli start well below threshold) or descending order (stimuli start well above threshold) and are presented until the perception of the subject changes. Since stimuli are presented in a monotonic fashion, there are chances that the subject expects the next stimulus also to be the same as the current one, leading to errors of habituation. Similarly, there are also chances that the subject understands that his perception is bound to change and could expect the next stimulus to be different from the present one, leading to errors of anticipation. So the psychophysical method used by Gundry to determine thresholds may have had an effect on his results. These errors can be overcome by presenting stimuli in a random fashion, rather than monotonically ascending or descending, another classical psychophysical method also known as the method of constant stimuli. But the disadvantage with this method is that it requires a large number of stimuli to arrive at thresholds and as discussed earlier, presenting a great many stimuli in vestibular testing is not practical.

So more recently researchers have employed adaptive psychophysical methods such as the staircase and PEST methods to avoid the shortcomings of the method-of-limits and reduce the number of stimuli required to reach thresholds. Investigators choose a

particular adaptive method based on the % of correct detection criterion they set for defining thresholds. The correct detection criterion depends on the psychophysical method chosen. Adaptive procedures are explained in detail in Leek (2001). For example, if a 1-down 1-up staircase was used it would target a threshold at which the subject is right 50% of the time. This is unacceptable as the subject could be just guessing. A 2-down 1-up staircase procedure would target a threshold at which the 70.7% of the time[1]- but this apparently has never been used. The 3-down 1-up staircase procedure employed by Grabherr et. al. (2008) targets a threshold at which the subject is right 79.4% of the time. Benson et. al. (1989) used an adaptive procedure and defined thresholds using a 75% correct detection criterion. The double staircase method presents two stimuli staircases to the subject – an ascending one (starting stimulus well below the estimated threshold) and a descending one (starting stimulus well above the estimated threshold). The two staircases cross-recross and finally zero-in on the threshold after a large number of trials (Cornsweet, 1962). However, for practical reasons, the staircases could be stopped after a predetermined number of trials after reaching the threshold plateau or after a predetermined number of reversals are obtained. For e.g., Grabherr et. al. (2008) stopped their testing after nine direction reversals were obtained and Benson et. al. after 50 trials were done. Therefore, experimenters have differed in their stopping criterion for the staircase methods and this will have an effect on the thresholds determined from the studies. But the differences may not be significant, because, by the time the staircase reaches 50 trials or 9 direction reversals, the administered stimuli may be really close to the threshold stimuli.

Almost all the vestibular threshold studies reviewed in this thesis measured **recognition thresholds** and not **detection thresholds**. Recognition thresholds are those that occur when two stimuli are presented to the subject (movement front or back, up or down, left or right) and the subject is forced to choose one of the options even if he/she is not certain about the direction or did not perceive motion. However, detection thresholds occur when subject is presented either with the stimulus or not, and the task of the subject is to detect the presence of the stimulus. Mah et. al. (1989) determined detection thresholds using a 2-interval forced-choice procedure. Only Benson et. al. (1986) allowed subjects to indicate if they did not perceive motion or were uncertain about the direction of it, thus not employing a forced-choice procedure. Assuming the same stimulus and same threshold criterion, the detection threshold should be at least twice the recognition threshold (Merfeld, 2010). (This theoretical relation is derived in more detail in Chapter 3.)

[1] [1]If p is the probability of positive response, then $p^2 = 0.5$ for a reduction in step size for 2-down 1-up staircase paradigm. This implies p = 0.707. Similarly, for the 3-down 1-up staircase paradigm, $p^3 = 0.5$ implies p = 0.794.

A recognition threshold paradigm has an advantage over a detection paradigm in that it does not depend on how certain the subject is that he felt motion. In contrast, a detection paradigm, the subject must decide how certain he wants to be that motion was felt. If he wants to minimize false detections, he is likely to use a high threshold. On the other hand he may want to please the experimenter by using a low threshold and report that he moved, risking the possibility of error. Because different subjects may adopt different levels of certainty, inter-subject variability becomes an issue. Direction recognition paradigms avoid these problems. Whatever direction recognition threshold the subject adopts, presumably it is the same in both directions. When both stimulus directions are administered, the subject is forced to choose one of them, regardless if he is not completely certain of the stimulus direction, or whether he even moved. Therefore, it is arguably better to conduct a recognition experiment than a detection experiment, and then estimate detection thresholds e.g. using a theoretical relationship (Merfeld, 2010 and explained later) such as doubling the thresholds obtained from the recognition experiment. Recognition experiments also overcome false sensations of motion caused by vibration cues, which could potentially affect detection experiments.. Although mathematically proven with certain assumptions (Merfeld, 2010), it is yet to be experimentally proved that the detection threshold is twice the recognition threshold.

3.3 EFFECT OF ORIENTATION WITH RESPECT TO GRAVITY

During horizontal linear acceleration, at a given frequency of oscillation, motion without direction is perceived for low stimulus magnitudes. As the magnitude of stimulus is increased, perception of direction arises and further increase in magnitude results in the perception of tilt (Guedry, 1974). For gravitationally vertical linear accelerations in the z axis, dorsoventral axis, subjects often misjudge motion direction. Literature shows that both angular and linear motions depend on the direction of motion with respect to gravity. Yaw motion thresholds are lower than pitch or roll motion thresholds, as is evident from Table 3.1 (Benson et. al, 1989). Linear motions along the dorsoventral z axis have higher thresholds than motions along the naso-occiptal x and interaural y axes, as seen from Table 3.2 (Benson et. al. 1986). To explain this behavior, Gundry (1978) hypothesized that, during horizontal movements (x and y axes), the linear acceleration acts in the plane of the utricular macula, and they might be more sensitive than the saccular macula. But physiological studies by Fernandez and Goldberg (1976) did not find any major differences in sensitivity between utricular and saccular maculae in squirrel monkey. It could be that humans simply process utricular information on acceleration better than saccular information, because most large amplitude linear movements when walking on Earth are in a horizontal plane. This difference in experience might lead to the difference in thresholds.

Angular motion thresholds are also affected by orientation of the subject with respect to gravity. Gundry (1978) found that roll thresholds were higher for subjects lying supine and rolled about a vertical axis than for subjects seated upright and rolled about a horizontal axis. He explained this behavior saying that the otoliths were also stimulated in the case of subjects being rolled about a horizontal axis, thus reducing the threshold. For subjects tested with a horizontal roll axis, he found that roll thresholds starting from an upright position were lower than those starting from a side-down position. Also thresholds from a side-down position to the inverted position were lower than the thresholds from a side-down position to the upright position. Gundry explained this behavior by suggesting that tilt perception was determined more by the change of the linear acceleration acting in the plane of the utricular macula than by that acting in the plane of the saccular macula.

The linear motion threshold study by Mah et. al. (1989) indicates that thresholds for linear motion are as low as 0.005 g's at low frequencies, which corresponds to a tilt of around 0.28 degrees. Hence, based on this, it might be possible for humans to sense tilts as low as this value. However, we know the threshold for tilt perception in the dark is way higher than this, typically 2- 6.5 degrees (e.g. Bringoux et. al., 2002). So this clearly indicates a discrepancy. This discrepancy could be explained by making use of the signal in noise model for thresholds. The fact that tilt thresholds are higher and don't correspond to 0.005 g's suggests that the noise in the perception of tilt is higher than the noise in the perception of linear motion. Therefore, it would require a larger tilt than 0.005 g's at this frequency to create a good enough tilt perceptual signal to noise ratio for detection, compared to the detection of linear motion.

3.4 OTHER FACTORS AFFECTING MOTION PERCEPTION THRESHOLDS

For threshold testing in the dark, to ensure that motion perception is based primarily on the vestibular organs, care should be taken to reduce or control other factors affecting motion perception. Padding around the head and body distributes forces and reduces the stimulus to proprioceptors in the skin. Also, restraining the head prevents Coriolis effects on the Semicircular Canals. Breeze cues are reduced by covering all skin surfaces, and using a visor. Auditory cues are usually masked by feeding white noise through ear phones or using ear muffs. For testing in the dark, visual cues are further minimized by by the use of light-occluding goggles or a blindfold, or testing in a darkened cab. Fatigue experienced by the subjects also affects the thresholds recorded from motion perception experiments. Scientists try to reduce subject fatigue by giving enough resting time between trials. Drowsiness experienced by the subject is very hard to control and also affects motion thresholds. When low frequency motion stimuli are presented to the

subjects for long durations, there are good chances of the subjects falling asleep and not paying attention to the stimulus, thus skewing the results. One method to keep the subjects awake is to alert them using the headphones that a stimulus is coming.

Vestibular and other health disorders could also affect thresholds. Scientists screen subjects by detailed vestibular diagnostic clinical examination to confirm the absence of any vestibular disorders. Some scientists also use caloric Electronystagmography, Hallpike testing and angular VOR testing in their screening process. These factors were well controlled by many of the researchers, for e.g. Benson et. al (1986 & 1989), Mah et. al (1989) and Grabherr et. al. (2008). Vibration cues are also essential to be controlled. Mah et. al. (1989) controlled vibration cues well by constructing an improved linear sled. However, Benson et. al. (1986 & 1989) stimuli included vibration, as is evident from their measurement of the input stimuli, Fig. 3.3. Such cues could have a huge impact on the results from detection threshold experiments. Gundry (1978) mentioned that some of the studies in his review demonstrated a mix of visual, auditory, somatic and proprioceptive sensory information for motion perception.

While the above are factors that can be controlled in a threshold testing experiment, there are others that cannot be controlled:

1) Past motion experience or stimulus knowledge of the subjects: The subjects might have prior knowledge from past motion experiences or gain knowledge during testing about the motion stimulus profiles they are presented with, and hence could influencing be skewing their threshold decision making.

2) Subject's age: An older subject's vestibular function will usually be less effective than a younger subject's (Snow et. al., 2009). Therefore, the subject's age is a factor in threshold testing whose effect can be reduced only if all the subjects are almost the same age. However, this would not give us an idea about the spectrum of vestibular thresholds, spanning all ages. Including subjects from a broad spectrum of ages in threshold studies, and if possible the effect of age should be quantified.

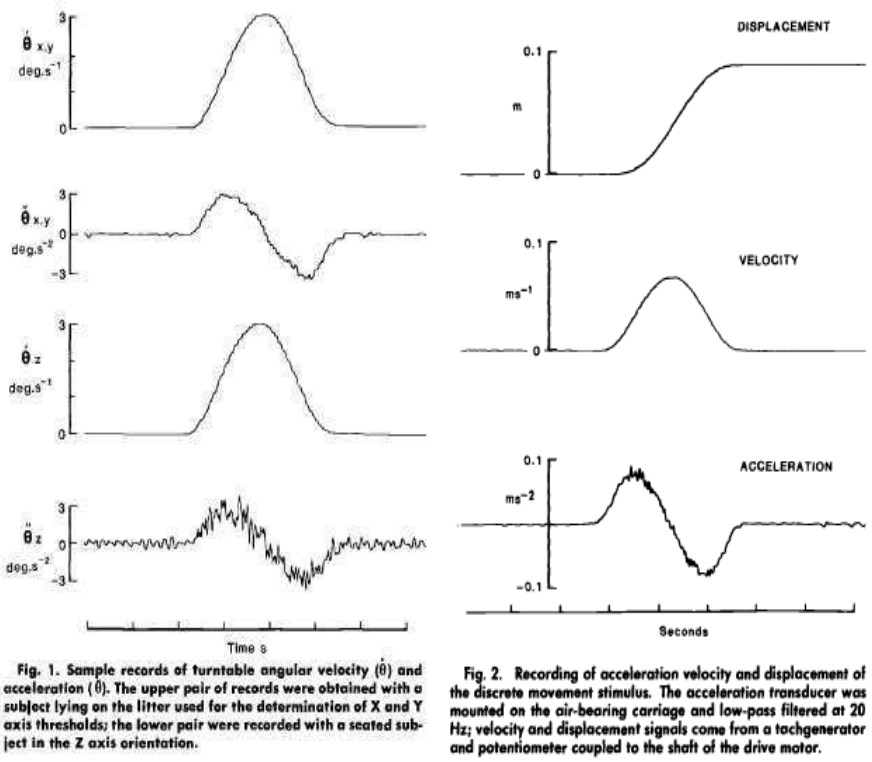

Fig. 1. Sample records of turntable angular velocity ($\dot{\theta}$) and acceleration ($\ddot{\theta}$). The upper pair of records were obtained with a subject lying on the litter used for the determination of X and Y axis thresholds; the lower pair were recorded with a seated subject in the Z axis orientation.

Fig. 2. Recording of acceleration velocity and displacement of the discrete movement stimulus. The acceleration transducer was mounted on the air-bearing carriage and low-pass filtered at 20 Hz; velocity and displacement signals come from a tachgenerator and potentiometer coupled to the shaft of the drive motor.

Fig. 3.3 – Input motion stimulus profiles adapted from Benson et. al. (1986 & 1989)

3) Inter-subject variability: Threshold values vary from person to person, and this is something that is not readily controllable, but important to understand.

From Table 3.1 & Table 3.2, it can be seen that thresholds for angular and linear motion perception in the literature vary by an order of magnitude. Most of the variation can be explained by the difference in motion stimulus profiles, difference in motion stimulus frequency and psychophysical methods used to determine thresholds. Benson et. al. (1986 & 1989), the other authors do not report the age of the subjects. So it is not clear if age was a factor in this variability. Benson et. al. tested subjects of age 20-49 and 20-46 respectively in their angular and linear threshold studies. It is to be remembered that most of the threshold testing is done under optimal conditions, where the only task of the subject is to sense motion. However, it has been demonstrated that motion perceptual thresholds are effectively raised when subjected are required to perform a mental arithmetic or vehicle steering task in addition (40% increase in roll thresholds) (Mah et. al., 1989). Conceivable some of the low threshold values in literature might have been due to improper control of stimulus during testing, allowing other sensory cues to contaminate the results. Whether the low threshold values from literature should be discarded or not depends on the case being considered and is difficult to assess.

Also, the other ‘good’ values for motion perception thresholds in the dark from the literature could be useful enough for clinical testing of subjects in the dark but are however not necessarily appropriate for flight simulator design, as flight simulators involve visual and other sensory cues too. So the thresholds in a flight simulator environment may be reduced by the presence of other sensory cues to vehicle motion, but also could be increased because the pilot is distracted by other complex tasks that he has to perform, or by the lack of relative visual motion of the cabin. Also, when the pilot is actively controlling the airplane, he would be aware when to attend motion cues, so that would also affect thresholds. Hence there is a competition between these factors in determining motion thresholds in a flight environment.

There are also certain questions regarding motion perception thresholds which the literature does not answer. The literature on pitch motion perception, roll motion perception and linear motion in a gravitational vertical direction is very limited. As these motion perceptions are not very well understood, any washout algorithms for pitch, roll and motion in a gravitational vertical direction is subject to error.

The effects of the knowledge and expectation of the subjects about motion perception testing and past motion experiences are factors that could be affecting motion perception thresholds, but are not well understood at this point. Also, there are problems relating to inter-subject variability. So with the current knowledge of thresholds, if a flight simulator washout is designed, it may work well for one subject but may fail for another. This presents a big challenge in simulator washout design.

CHAPTER 4: MATCHED FILTER MODEL FOR YAW THRESHOLDS

While Chapter 3 dealt with motion perception thresholds in general, the rest of the Chapters in the thesis are focused on the challenge of modeling yaw thresholds in the dark. It was noted earlier that a widely accepted threshold modeling concept is the "signal in noisy perceptions" approach. The models developed assumed this, and were matched with the data from the most comprehensive and recent study on yaw recognition thresholds performed by Grabherr et. al. (2008). They had determined yaw thresholds for single cycle sinusoidal acceleration stimuli of varying frequency using a forced-choice procedure and 3-down 1-up staircase algorithm. This psychophysical method targets a threshold at which correct prediction of motion direction occurs 79.4% of the time. Since they never used the 'no motion' condition in their study and the subjects were always rotated in one direction or the other, the threshold values from the paper are recognition thresholds, as explained in Chapter 3.

Now, getting back to the dependence of thresholds on the motion stimulus profile, the behavior of motion thresholds for constant acceleration stimuli is hypothesized as follows:

When any constant acceleration stimulus is input to the subject for **infinite** duration, the actual angular velocity keeps linearly increasing, but the response of the Semicircular Canal (SCC) signal increases approximately linearly only for durations shorter than the canal time constant. Thereafter, the cupula exponentially converges to a constant deflection and afferent response and rotation sensation decline. The peak response of the SCC output depends on the value of the acceleration stimulus and the sensation of rotation is in turn dependent on the peak value of the SCC output. Therefore, it is hypothesized that to create a perceivable sensation of rotation amidst noise, the acceleration has to be a minimum value, which is the threshold value. Even at low signal to noise ratios, it may still be possible to perceive rotation, but the consistency of detection (e.g., how many times a subject gets the direction right out of 100 times the same stimulus is presented) can be much lower than 100%. That is why Benson et. al. (1986 & 1989) and Grabherr et. al. (2008) defined their thresholds in a probabilistic sense – percentage of times a subject correctly detects the correct direction of the stimulus.

While the signal in noisy perception hypothesis can partly explain the behavior of motion thresholds for constant accelerations, they can only partly explain the behavior of motion thresholds for sustained and single cycle sinusoidal stimuli. If the maximum perceived velocity reached during a sinusoidal acceleration stimulus always remains within a

certain value, no matter how high the frequency of the stimulus is, the perceived velocity to noise ratio may not be sufficient for motion perception. This explains the existence of a plateau in the case of yaw velocity thresholds as shown in Fig. 4.1, found from the study by Grabherr et. al (2008). This plateau essentially means that no matter what the frequency of the stimulus is, the peak velocity reached during the stimulus should be a minimum value before it is perceived (0.71 deg.s^{-1} in this case). However, if the peak velocity reached during the sinusoidal acceleration stimulus is above this minimum value, thresholds become a function of frequency. This behavior can be explained by the following hypothesis:

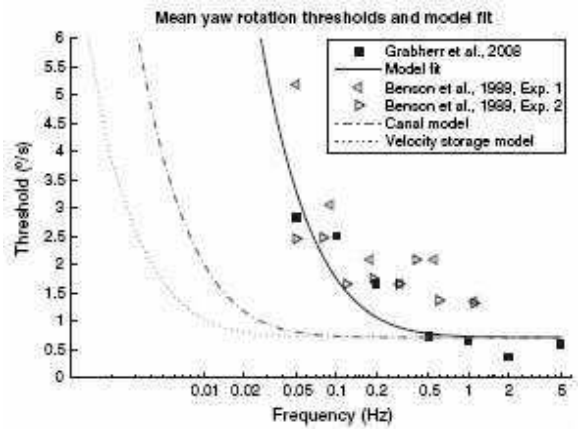

Fig. 4.1 – Velocity (Peak velocity) thresholds for yaw motion as a function of frequency – adapted from Grabherr et. al. 2008

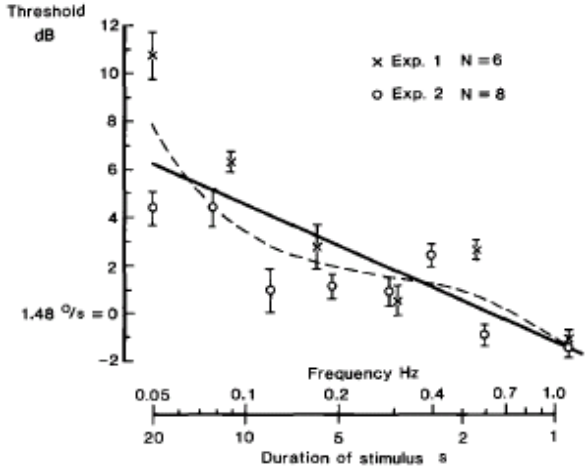

Fig. 4.2 – Velocity (Peak velocity) thresholds for yaw motion as a function of frequency – adapted Benson et. al. 1989

It is quite possible that humans have a vague idea of the bandwidth and amplitude of their perceptual noise. It is assumed here that the subject perceives the velocity of the stimulus

and also the rate of change of the perceived velocity signal (perceived acceleration). Therefore, noise in perceived velocity causes false perceptions of acceleration, but these accelerations are limited in magnitude because of the bandwidth and maximum amplitude of the perceptual noise. Therefore, when the frequency of the stimulus is high, even if the global peak velocity perceived during the stimulus is low, the global peak acceleration perceived during the stimulus will be higher than that possible by pure noise. However, there would need to be a minimum peak velocity so that the signal to noise ratio is good enough for telling the stimulus. This accounts for the existence of a plateau for higher frequencies. But at low frequencies, the global peak acceleration reduces for the same global peak velocity. This means that the accelerations perceived during the stimulus may not be very different from the ones possible by only noise. Hence to distinguish the stimulus from noise better, the global peak velocity perceived during the stimulus should be high and hence the threshold increases.

In the following sections, the relation between thresholds for recognition and detection tasks will be derived.

4.1 RECOGNITION THRESHOLD

To determine the recognition threshold for yaw motion, the subject is either rotated to the left or to the right and asked to predict the direction of rotation. When rotated, the subject's semicircular canals respond to this rotation and send afferents to the central nervous system, which results in a perception of rotation. However, these afferent signals are affected by neural noise which in turn causes uncertainty (noise) in the perceived velocity. For the recognition task, the subject is forced to associate this perceived noisy velocity with rotation in one direction or the other. The recognition task can therefore be formulated as a statistical hypothesis testing problem with the following null and alternate hypotheses:

$$\begin{aligned} H_0 &: x[n] = -As[n] + w[n] \quad \sim \text{Left Rotation} \\ H_1 &: x[n] = As[n] + w[n] \quad \sim \text{Right Rotation} \end{aligned} \qquad n = 0,1,...,N-1 \quad (4.1)$$

where $x[n]$ – perceived velocity corrupted by noise
$s[n]$ – 'noise-free' perceived velocity corresponding to a unit amplitude single cycle sinusoidal acceleration stimulus towards right
$w[n]$ – noise in perceived velocity, assumed to be White Gaussian noise with mean 0 and standard deviation σ; $w[n] \sim N(0,\sigma^2)$

Here, based on the method used in Grabherr's recognition threshold experiment it is assumed that the subject knows the frequency and waveform of the stimulus s[n] used in

the trial, and only the amplitude A of the signal is unknown. The subject is assumed to use discrete samples of perception to make his decision. Since $s[n]$ corresponds to rotation to the right for a unit amplitude acceleration stimulus, $As[n]$ corresponds to rotation towards right and - $As[n]$ corresponds to rotation towards left for an acceleration stimulus of amplitude A.

For this symmetric recognition problem, subject who was estimating the likelihood of the signal being present would associate a perceived velocity $\mathbf{x} = x[n]$, $n = 0,1,...,N-1$, with rotation towards right if

$$\frac{p(\mathbf{x};H_1)}{p(\mathbf{x};H_0)} > 1 \qquad (4.2)$$

The noise in angular velocity perceptions presumably originates from variations in the semicircular canal afferent firing rates (i.e. measurement noise). Its bandwidth will be influenced by CNS processing that determines the perception (e.g. the dynamics of central velocity storage.) The noise is assumed to be Gaussian. Based on detection theory as developed by Kay (1998) Equation (4.2) becomes

$$\frac{\frac{1}{\left(2\pi\sigma^2\right)^{\frac{N}{2}}}\exp\left[-\frac{1}{2\sigma^2}\sum_{n=0}^{N-1}\left(x[n]-As[n]\right)^2\right]}{\frac{1}{\left(2\pi\sigma^2\right)^{\frac{N}{2}}}\exp\left[-\frac{1}{2\sigma^2}\sum_{n=0}^{N-1}\left(x[n]+As[n]\right)^2\right]} > 1$$

or

$$\exp\left[-\frac{1}{2\sigma^2}\sum_{n=0}^{N-1}\left(-4Ax[n]s[n]\right)\right] > 1$$

Taking logarithms and simplifying yields,

$$A\sum_{n=0}^{N-1}x[n]s[n] > 0 \qquad (4.3)$$

In other words, for the recognition problem, the subject makes the decision that he is turning to the right if equation (4.3) holds. Otherwise, the subject makes the decision that he is turning to the left.

We note that the statistic $u(\mathbf{x}) = A\sum_{n=0}^{N-1} x[n]s[n]$ follows normal distributions with the following different parameters under H_0 and H_1.

$$u(\mathbf{x}) = A\sum_{n=0}^{N-1} x[n]s[n] \sim \begin{cases} N\left(-A^2\sum_{n=0}^{N-1} s^2[n], A^2\sigma^2\sum_{n=0}^{N-1} s^2[n]\right) & \sim H_0 \\ N\left(A^2\sum_{n=0}^{N-1} s^2[n], A^2\sigma^2\sum_{n=0}^{N-1} s^2[n]\right) & \sim H_1 \end{cases}$$

In Fig. 4.3, the normal distributions of $u(\mathbf{x})$ corresponding to left (blue) and right (red dashed) rotations with mean μ = 0.82 and standard deviation σ = 1 are shown . The corresponding cumulative probability distributions for $u(\mathbf{x})$ is shown in Fig. 4.4. From equation (4.3), we find that the subject would choose motion to the right if $u(\mathbf{x})$>0. If the investigator defined the probability of correct prediction of rotation towards right required as 79.4% correct, as in Grabherr's case, after transforming $u(\mathbf{x})$ to a standard normal variable, from Fig. 4.3, we have,

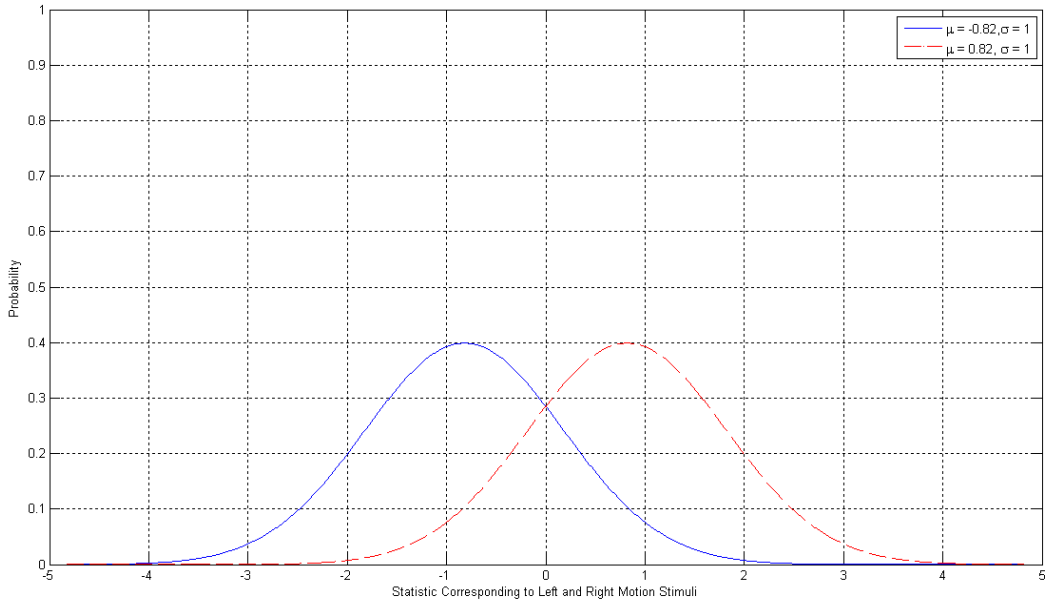

Fig. 4.3 – Probability distribution functions of the statistic corresponding to the left and right motion stimuli

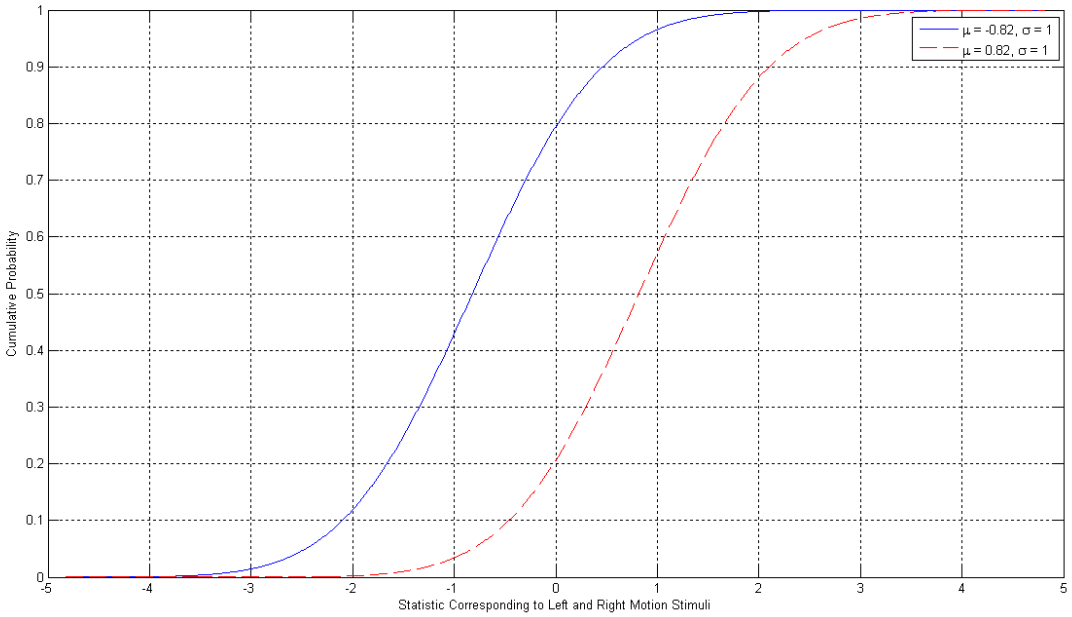

Fig. 4.4 – Cumulative Probability distribution functions of the statistic corresponding to the left and right motion stimuli

$$1-Q\left(\frac{\left(0-\left(-A_{rec}{}^{2}\sum_{n=0}^{N-1}s^{2}[n]\right)\right)}{\sqrt{A_{rec}{}^{2}\sigma^{2}\sum_{n=0}^{N-1}s^{2}[n]}}\right)=0.794$$

or,

$$\frac{\left(0-\left(-A_{rec}{}^{2}\sum_{n=0}^{N-1}s^{2}[n]\right)\right)}{\sqrt{A_{rec}{}^{2}\sigma^{2}\sum_{n=0}^{N-1}s^{2}[n]}}=0.82$$

where $Q(x)=\frac{1}{\sqrt{2\pi}}\int_{x}^{\infty}e^{\frac{x^{2}}{2}}dx$ and A_{rec} is the amplitude of the recognition threshold stimulus.

The equation reduces to,

$$\frac{A_{rec}}{\sigma}\sqrt{\sum_{n=0}^{N-1}s^{2}[n]}=0.82 \qquad (4.4)$$

Equation (4.4) shows the relation between the amplitude of the recognition threshold stimulus, noise-free perceived velocity $\boldsymbol{s} = s[n]$, $n = 0,1,...,N-1$, and standard deviation of

the noise in perceived velocity σ. Note that this result depends only on the probability of correct direction recognition as defined by the investigator. Assuming the responses in the two directions are symmetrical, it is independent of how certain the subject himself is trying to be, e.g. whether the subject intended to be correct 79.4% or 90% of the time.

4.2 DETECTION THRESHOLD

To determine the corresponding detection threshold for yaw motion, the subject is either rotated or held static. So the subject's task is to predict if he has been rotated or not. In other words, the subject has to associate his perceived noisy velocity with either a stimulus or just noise. The detection problem can therefore be formulated as a statistical hypothesis testing problem with the following null and alternate hypotheses:

$$\begin{aligned} H_0 &: x[n] = w[n] && \sim \text{No Rotation} \\ H_1 &: x[n] = As[n] + w[n] && \sim \text{Right Rotation} \end{aligned} \qquad n = 0,1,\ldots,N-1 \quad (4.5)$$

(In this case, we have only considered rotation to the right, but the same condition is valid if the experiment was performed using rotations to the left). The subject is assumed to associate a perceived velocity $\mathbf{x} = x[n]$, $n = 0,1,\ldots,N-1$, with rotation towards right if

$$\frac{p(\mathbf{x};H_1)}{p(\mathbf{x};H_0)} > \gamma \qquad (4.6)$$

where γ could be any value and not necessarily 1, unlike the symmetric recognition problem. The value of γ, also known as the **criterion bias**, is assumed chosen by the subject based on the pay-offs and costs associated with correct detection and false alarms. Again following the development in Kay (1998) , and assuming Gaussian noise, Equation (4.6) becomes

$$\frac{\frac{1}{\left(2\pi\sigma^2\right)^{\frac{N}{2}}}\exp\left[-\frac{1}{2\sigma^2}\sum_{n=0}^{N-1}\left(x[n]-As[n]\right)^2\right]}{\frac{1}{\left(2\pi\sigma^2\right)^{\frac{N}{2}}}\exp\left[-\frac{1}{2\sigma^2}\sum_{n=0}^{N-1}x^2[n]\right]} > \gamma$$

or,

$$\exp\left[-\frac{1}{2\sigma^2}\sum_{n=0}^{N-1}\left(-2Ax[n]s[n]+A^2s^2[n]\right)\right] > \gamma$$

Taking logarithms,

$$-\frac{1}{2\sigma^2}\sum_{n=0}^{N-1}\left(-2Ax[n]s[n]+A^2s^2[n]\right)>\ln\gamma$$

or,

$$A\sum_{n=0}^{N-1}x[n]s[n]>\sigma^2\ln\gamma+\frac{A^2}{2}\sum_{n=0}^{N-1}s^2[n]=\gamma' \qquad (4.7)$$

We note that the statistic $u(\mathbf{x})=A\sum_{n=0}^{N-1}x[n]s[n]$ follows normal distributions with the following different parameters under H_0 and H_1.

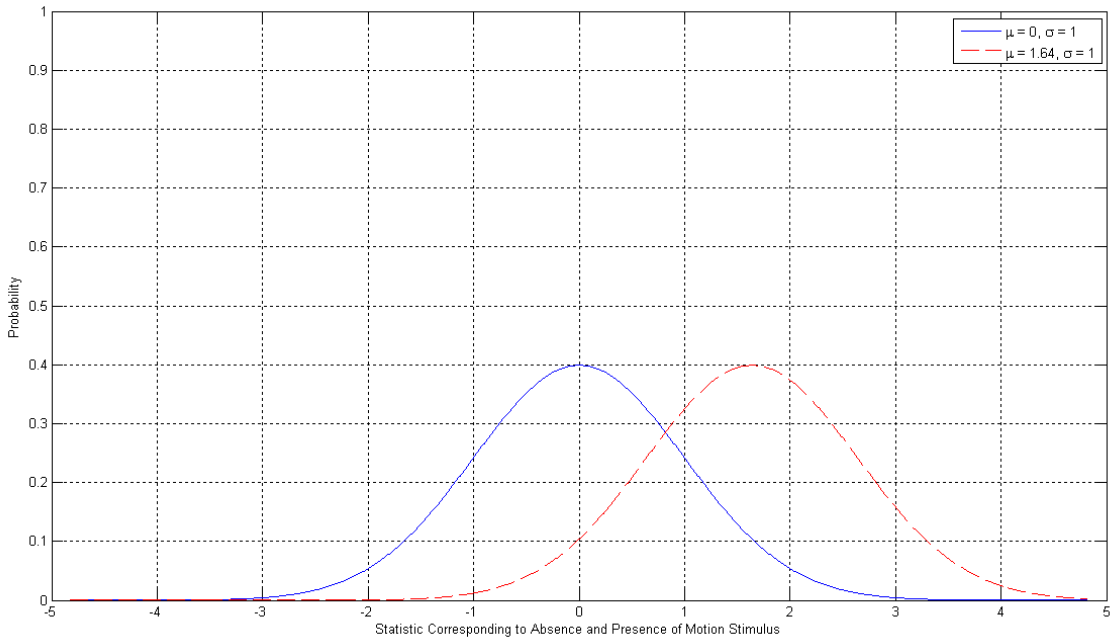

Fig. 4.5 – Probability distribution functions of the statistic corresponding to the absence and presence of motion stimulus

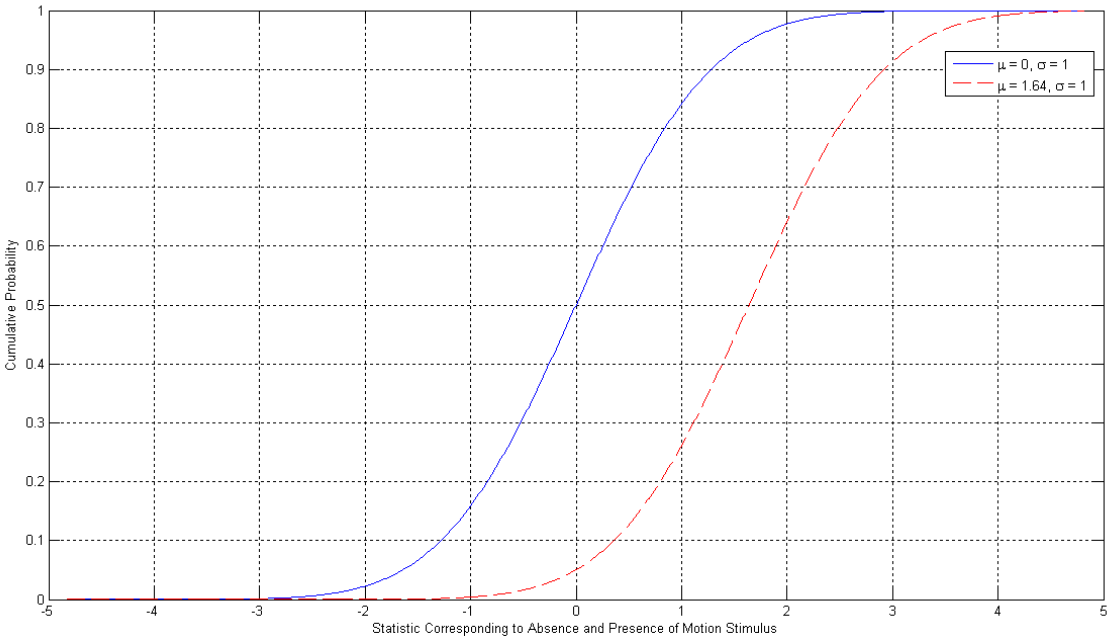

Fig. 4.6 – Cumulative probability distribution functions of the statistic corresponding to the absence and presence of motion stimulus

$$u(\mathbf{x}) = A\sum_{n=0}^{N-1} x[n]s[n] \sim \begin{cases} N\left(0, A^2\sigma^2\sum_{n=0}^{N-1} s^2[n]\right) & \sim H_0 \\ N\left(A^2\sum_{n=0}^{N-1} s^2[n], A^2\sigma^2\sum_{n=0}^{N-1} s^2[n]\right) & \sim H_1 \end{cases} \tag{4.8}$$

In Fig. 4.5, the normal distributions of $u(\mathbf{x})$ corresponding to no rotation (blue) and rotation to the right (red dashed) with mean μ = 1.64 and standard deviation σ = 1 are shown

Fig. 4.6 shows the corresponding cumulative probability distributions for $u(\mathbf{x})$. From equation (4.7), we find that the subject would decide he is moving if $u(\mathbf{x}) > \gamma'$. For purposes of illustration, let us assume the subject decided he wanted the probability of correct detection of rotation to be 79.4% (in this case the same criterion adopted by the investigator when scoring). After transforming $u(\mathbf{x})$ to a standard normal variable, from Fig. 4.5, we have,

$$P_D = \Pr\{u(\mathbf{x}) > \gamma'; H_1\} = 0.794$$

$$\Rightarrow Q\left(\frac{\gamma' - {A_{\text{det}}}^2 \sum_{n=0}^{N-1} s^2[n]}{\sqrt{{A_{\text{det}}}^2 \sigma^2 \sum_{n=0}^{N-1} s^2[n]}}\right) = 0.794$$

$$\Rightarrow \frac{\left(\gamma' - {A_{\text{det}}}^2 \sum_{n=0}^{N-1} s^2[n]\right)}{\sqrt{{A_{\text{det}}}^2 \sigma^2 \sum_{n=0}^{N-1} s^2[n]}} = -0.82$$

where $Q(x) = \frac{1}{\sqrt{2\pi}} \int_x^\infty e^{-\frac{x^2}{2}} dx$ and A_{det} is the amplitude of the detection threshold stimulus.

For purposes of this example, we will also assume that the subject's acceptable probability of false detection is 1- P(correct detection) = 20.6%. After transforming $u(\mathbf{x})$ to a standard normal variable, from Fig. 4.5, we have,

$$P_{FA} = \Pr\{u(\mathbf{x}) > \gamma'; H_0\} = 0.206$$

$$\Rightarrow Q\left(\frac{\gamma'}{\sqrt{{A_{\text{det}}}^2 \sigma^2 \sum_{n=0}^{N-1} s^2[n]}}\right) = 0.206$$

$$\Rightarrow \frac{\gamma'}{\sqrt{{A_{\text{det}}}^2 \sigma^2 \sum_{n=0}^{N-1} s^2[n]}} = 0.82$$

$$\Rightarrow \gamma' = 0.82\sqrt{{A_{\text{det}}}^2 \sigma^2 \sum_{n=0}^{N-1} s^2[n]}$$

Substituting the value of γ' in the condition from $P_D = 0.794$, we have,

$$\frac{\left(\gamma' - {A_{\text{det}}}^2 \sum_{n=0}^{N-1} s^2[n]\right)}{\sqrt{{A_{\text{det}}}^2 \sigma^2 \sum_{n=0}^{N-1} s^2[n]}} = -0.82$$

$$\Rightarrow \frac{\left(0.82\sqrt{{A_{\text{det}}}^2 \sigma^2 \sum_{n=0}^{N-1} s^2[n]} - {A_{\text{det}}}^2 \sum_{n=0}^{N-1} s^2[n]\right)}{\sqrt{{A_{\text{det}}}^2 \sigma^2 \sum_{n=0}^{N-1} s^2[n]}} = -0.82$$

$$\Rightarrow 0.82 - \frac{A_{\text{det}}}{\sigma}\sqrt{\sum_{n=0}^{N-1} s^2[n]} = -0.82$$

$$\Rightarrow \frac{A_{\text{det}}}{\sigma}\sqrt{\sum_{n=0}^{N-1} s^2[n]} = 1.64 \qquad (4.9)$$

Equation (4.9) shows the relation between the amplitude of the detection threshold stimulus, noise-free perceived velocity $\boldsymbol{s} = s[n]$, $n = 0,1,...,N-1$, and standard deviation of the noise in perceived velocity σ. Dividing equation (4.9) by equation (4.4), we have,

$$\frac{A_{\text{det}}}{A_{rec}} = 2 \qquad (4.10)$$

Therefore, for the values of P(correct detection) and P(false detection) assumed by the subject the amplitude of the detection threshold stimulus is twice that of the recognition threshold stimulus.vIf the subject were penalized more for making a false alarm, his criterion bias would change, and therefore, the detection threshold also changes. By varying the penalty, the subject can be moved along a ROC (Receiver Operating Characteristics) curve, and different detection thresholds would be obtained in each case, and the relationship between A_{det} and A_{rec} would change. But for the remainder of the sections in the thesis, it is assumed that the detection threshold is twice the recognition threshold.

4.3 DETERMINING DETECTION THRESHOLDS FROM GRABHERR'S STUDY

The equation for the single cycle sinusoidal acceleration employed in Grabherr's study can be written as

$$a(t) = A\sin(2\pi ft) \qquad 0 < t < \frac{1}{f} \qquad (4.11)$$

where A is the amplitude and f is the frequency of the sinusoidal stimulus. $A > 0$ means rotation to the right, and $A < 0$ means rotation to the left.

This acceleration stimulus corresponds to a cosine-bell velocity of the form

$$v(t) = \frac{A}{2\pi f}\left(1 - \cos(2\pi ft)\right) \qquad (4.12)$$

From equations (4.11) and (4.12), we find that

$$a_{peak} = A \qquad (4.13)$$

$$v_{peak} = \frac{A}{\pi f} \qquad (4.14)$$

Grabherr et. al. (2008) proposed a "high pass filter" model for recognition thresholds (assuming a 79.4% correct prediction criterion) expressed using peak velocity as a function of frequency as

$$v_{peak} = \frac{1}{K} + \frac{1}{K\tau s} \qquad (4.15)$$

Where, $\frac{1}{K} = 0.71$ deg. s^{-1}, $\tau = 0.70$ s and $s = 2\pi f$, f is the frequency of the stimulus.

Frequency f Hz	**Peak Velocity V_{peak} deg. s^{-1}**	**Amplitude of the Recognition Threshold Acceleration Stimulus A_{rec} deg. s^{-2}**	**Amplitude of the Detection Threshold Acceleration Stimulus A_{det} deg. s^{-2}**
0.05	3.9386	0.6187	1.2373
0.1	2.3243	0.7302	1.4604
0.2	1.5171	0.9532	1.9065
0.5	1.0329	1.6224	3.2448
1	0.8714	2.7377	5.4753
2	0.7907	4.9682	9.9364
5	0.7423	11.6598	23.3196

Table 4.1 – A_{det} vs f

From (4.14), the peak velocity attained at recognition threshold is given by,

$$v_{peak} = \frac{A_{rec}}{\pi f} \qquad (4.16)$$

Therefore, by combining equations (4.10), (4.15) and (4.16), A_{det} as a function of frequency can be calculated as shown in Table 4.1 above.

4.4 ASSUMPTION ON σ

The recognition threshold values for frequencies > 2 Hz from Grabherr's data suggest that if a subject tries to be 79.4% correct, the corresponding detection threshold should be about 1.42 deg. s^{-1}. It was assumed that this is the uncertainty associated with the perceived velocity, and the subject had to experience a velocity greater than this uncertainty to correctly detect motion. A normal distribution for the uncertainty was assumed, and for a normal distribution, the probability that the normal variable takes a value between +/- σ is 68.2%. Hence to be more than 68.2% sure that motion existed, σ, the standard deviation of noise in perceived velocity was chosen to be 1.42 deg.s^{-1}.

4.5 MATCHED FILTER FOR THRESHOLDS

In the case of Grabherr's experiment, the waveform of the stimuli is assumed known to the subject, so it was thought of constructing a matched filter to model the experiment. A matched filter correlates a known signal or template (in this case, $A\mathbf{s}$) with an unknown signal (in this case, $\mathbf{x}$), to detect the presence of the template in the unknown signal. If σ, A_{det} and $\mathbf{s} = s[n]$, $n=0,1,...,N-1$ as a function of frequency are known, it is possible to construct this matched filter.

The detector designed here explicitly assumes that it has knowledge of $\mathbf{s} = s[n]$, $n=0,1,...,N-1$ in equation (4.1). The signal $\mathbf{s}$ is the sampled output of perceived angular velocity from the CNS *Observer* when the sinusoidal acceleration stimulus is input into it.

In the case of a subject experiencing a general motion stimulus, the frequency of the stimulus is often unknown. However, in the case of Grabherr's experiment, all trials in a given staircase were at the same frequency and the subjects were asked to respond only after the sinusoidal acceleration stimulus was administered. Particularly after several suprathreshold stimuli, the subjects likely knew the frequency content of the stimulus. Therefore, the perceived noisy velocity $\mathbf{x} = x[n]$, $n=0,1,...,N-1$ is available as input to the detector as soon as the stimulus is administered. So, the frequency of the stimulus can be estimated as

$$f = \frac{1}{duration} \quad (4.17)$$

where *duration* is the duration of the stimulus. Using Table 4.1, the detection threshold stimulus amplitude value A_{det} for this frequency f is found using interpolation. The corresponding $\mathbf{s} = s[n]$, $n=0,1,...,N-1$ is obtained by inputting a unit amplitude single cycle sinusoidal acceleration stimulus of frequency f to *Observer* and sampling its output. For the model built, a sampling rate of 15 Hz was used. The sampling frequency can be changed, but depends on the signal and noise bandwidths. To obtain the perceived noisy velocity signal $\mathbf{x} = x[n]$, $n=0,1,...,N-1$, Gaussian noise of variance $\sigma = 1.42$ deg.s^{-1} was added to **s**.

Now, as explained in Section 4.2, the detector decides that a stimulus exists if,

$$\frac{p(\mathbf{x};H_1)}{p(\mathbf{x};H_0)} > \gamma$$

where H_1 is the hypothesis that the stimulus exists, and H_0 is the hypothesis that there is no signal. With the assumed Gaussian noise, this inequality becomes,

$$\frac{\frac{1}{\left(2\pi\sigma^2\right)^{\frac{N}{2}}}\exp\left[-\frac{1}{2\sigma^2}\sum_{n=0}^{N-1}\left(x[n]-As[n]\right)^2\right]}{\frac{1}{\left(2\pi\sigma^2\right)^{\frac{N}{2}}}\exp\left[-\frac{1}{2\sigma^2}\sum_{n=0}^{N-1}x^2[n]\right]} > \gamma$$

or,

$$\exp\left[-\frac{1}{2\sigma^2}\sum_{n=0}^{N-1}\left(-2Ax[n]s[n]+A^2s^2[n]\right)\right] > \gamma$$

Taking logarithms,

$$-\frac{1}{2\sigma^2}\sum_{n=0}^{N-1}\left(-2Ax[n]s[n]+A^2s^2[n]\right) > \ln\gamma \quad (4.18)$$

Now, only the frequency of the stimulus in a trial can be estimated, but the amplitude A is unknown, the maximum likelihood estimate of the amplitude A, $\hat{A}$ is used,

$$\text{where, } \hat{A} = \frac{\sum_{n=0}^{N-1}x[n]s[n]}{\sum_{n=0}^{N-1}s^2[n]}$$

This derivation too is based on the development by Kay (1998). Therefore, (4.18) becomes,

$$-\frac{1}{2\sigma^2}\sum_{n=0}^{N-1}\left(-2\hat{A}x[n]s[n]+\hat{A}^2s^2[n]\right)>\ln\gamma$$

Substituting for $\hat{A}$, we get,

$$T(\mathbf{x})=\left(\sum_{n=0}^{N-1}x[n]s[n]\right)^2>2\sigma^2\ln\gamma\sum_{n=0}^{N-1}s^2[n]=\gamma'$$

or,

$$\left|\sum_{n=0}^{N-1}x[n]s[n]\right|>\sqrt{\gamma'}$$

Now, if we consider just positive rotations (negative rotations are symmetric and hence the results will be similar), the detector computes the statistic $T(\mathbf{x})=\sum_{n=0}^{N-1}x[n]s[n]$. The statistic $T(\mathbf{x})$ follows a normal distribution with the following parameters under H_0 and H_1.

$$T(\mathbf{x})=\sum_{n=0}^{N-1}x[n]s[n]\sim\begin{cases}N\left(0,\sigma^2\sum_{n=0}^{N-1}s^2[n]\right) & \sim H_0\\ N\left(A\sum_{n=0}^{N-1}s^2[n],\sigma^2\sum_{n=0}^{N-1}s^2[n]\right) & \sim H_1\end{cases} \qquad (4.19)$$

We assume the subject desires the probability of correct detection be 79.4% when the stimulus is of threshold intensity, i.e. when $A = A_{\text{det}}$,

$$P_D = \Pr\left\{u(\mathbf{x}) > \sqrt{\gamma}'; H_1\right\} = 0.794$$

$$\Rightarrow Q\left(\frac{\sqrt{\gamma}' - A_{\text{det}}\sum_{n=0}^{N-1} s^2[n]}{\sqrt{\sigma^2\sum_{n=0}^{N-1} s^2[n]}}\right) = 0.794$$

$$\Rightarrow \frac{\left(\sqrt{\gamma}' - A_{\text{det}}\sum_{n=0}^{N-1} s^2[n]\right)}{\sqrt{\sigma^2\sum_{n=0}^{N-1} s^2[n]}} = -0.82$$

$$\Rightarrow \sqrt{\gamma}' = -0.82\sigma\sqrt{\sum_{n=0}^{N-1} s^2[n]} + A_{\text{det}}\sum_{n=0}^{N-1} s^2[n] \qquad (4.20)$$

where $\sqrt{\gamma}'$ is the threshold for the statistic $T(\mathbf{x})$ to decide if the stimulus is present or not.

For negative rotations, the criterion would be $T(\mathbf{x}) < -\sqrt{\gamma}'$

Therefore, the detector will decide that a stimulus exists if,

$$\left|T(\mathbf{x})\right| = \left|\sum_{n=0}^{N-1} x[n]s[n]\right| \geq -0.82\sigma\sqrt{\sum_{n=0}^{N-1} s^2[n]} + A_{\text{det}}\sum_{n=0}^{N-1} s^2[n] \quad (4.21)$$

Since this model for detection compares how closely $x[n]$ matches $s[n]$ through the product $\left|\sum_{n=0}^{N-1} x[n]s[n]\right|$ and comparing it with a threshold value, this model is termed as the "Matched Filter Detector Model for Thresholds".

The matched filter model can be schematically represented as shown below

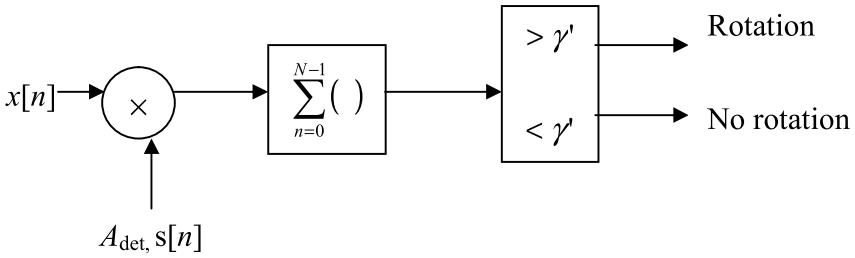

Fig. 4.7 – Matched Filter Detector Model for Thresholds

The biggest drawbacks of the matched-filter threshold model for yaw perception are that it assumes the subject knows the waveform of the perceived stimulus, and strictly speaking it should not be applied for stimuli other than single cycle sinusoids of acceleration. This model assumes that the subject has an idea of when the stimulus will be applied and how long will it last, which was true in the case of Grabherr's experiment.

A matched-filter detector model for thresholds was constructed in MATLAB as described above. The detector took the output **s** from *Observer* added with noise **x** as input, and estimated the frequency of the stimulus and A_{det} for that frequency. Then, it matched **x** with signal **s**. For example, for the 0.05 Hz sinusoidal acceleration stimulus, the noise-free perceived yaw velocity **s** would be as shown in Fig. 4.8.

Note that in Fig. 4.8, **s** is different from the actual angular velocity, due to the SCC and velocity storage dynamics of *Observer*. The form of **s** changes with the frequency and type of stimulus. So the method to set up the matched-filter model for thresholds to detect a single cycle sinusoidal acceleration stimulus of amplitude A is as follows:

1) Run *Observer* with a unit amplitude single cycle sinusoidal acceleration stimulus of that frequency. The perceived yaw velocity output from *Observer* is the signal **s** for that stimulus.

2) Now, add noise of $\sigma = 1.42$ deg.s^{-1} to A**s.** This is the perceived noisy yaw velocity **x** for that stimulus.

3) Estimate the frequency and A_{det} of the input stimulus. Using **x**, **s** and A_{det}, calculate $T(\mathbf{x})$ and $\sqrt{\gamma'}$.

4) If $T(\mathbf{x}) \geq \sqrt{\gamma'}$, the stimulus will be detected.

The above model was tested with all the stimuli used in Grabherr's study. The performance of the model is discussed later in detail in Chapter 6.

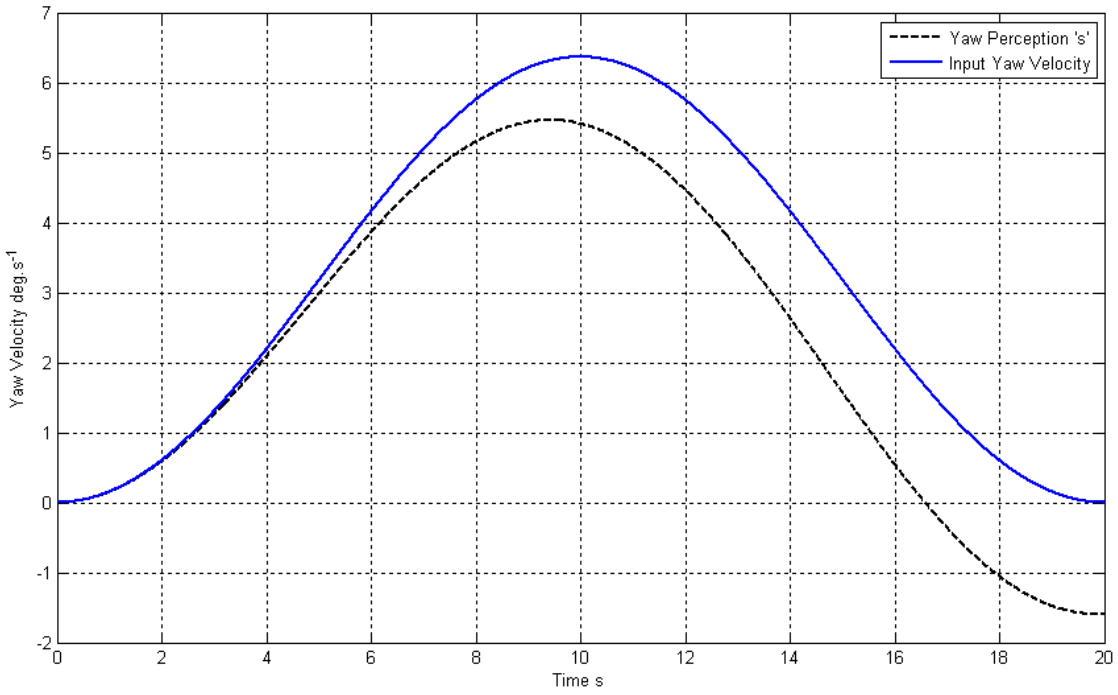

Fig. 4.8 – Noise-free perceived velocity **s** and the actual velocity for a unit amplitude sinusoidal acceleration stimulus of 0.05 Hz

CHAPTER 5: TWO-THRESHOLD MODEL FOR YAW PERCEPTION

As noted earlier Matched-Filter model is only appropriate for single sinusoidal stimuli and is useful in detecting motion only **after** the motion stimulus is completely administered. Therefore, it cannot be used to model the detection of motion **during the course** of motion, and hence is not particularly appropriate for predicting spatial disorientation illusions. The Two-Threshold model for yaw motion developed below is an attempt to develop a model for detection motion during course of the motion stimulus. This model is based on a trend noted by Grabherr et al that the yaw threshold values reported by Grabherr et. al. increase as a function of frequency is shown in Fig. 4.1. The study revealed the existence of a plateau for frequencies above 0.5 Hz. This plateau was 0.71 deg.s^{-1} for recognition, which – given the assumptions regarding subject detection bias detailed in the previous chapter – corresponds to 1.42 deg.s^{-1} for detection threshold.

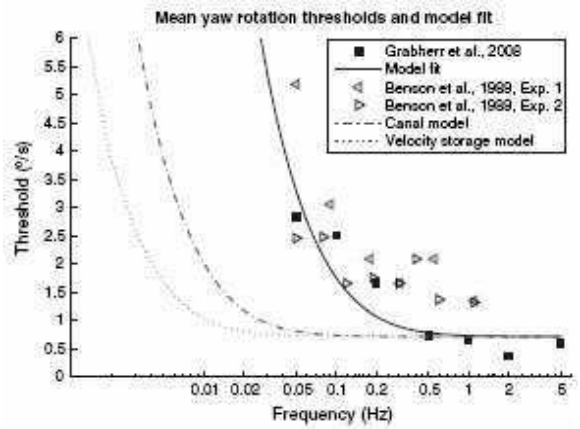

Fig. 4.1 – Velocity (Peak velocity) thresholds for yaw motion as a function of frequency – adapted from Grabherr et. al. 2008

In other words, if the peak velocity attained is $\geq v_{thresh}$ = 1.42 deg.s^{-1} and if the frequency of the stimulus is $\geq$ 0.5 Hz, the subject would correctly detect motion 79.4% of the time. However, if the frequency of the stimulus is < 0.5 Hz, this velocity threshold increases with decreasing frequency and is not a constant.

The peak accelerations for these detection threshold stimuli, adapted from Table 4.1 are shown in Table 5.1.

Frequency Hz	**Peak Angular Acceleration deg.s^{-2}**
0.05	1.2373
0.1	1.4604

0.2	1.9065
0.5	3.2448
1	5.4753
2	9.9364
5	23.3196

Table 5.1 – Peak acceleration values for detection threshold stimuli calculated from Grabherr's data

The peak acceleration values below 0.5 Hz show that they are almost a constant ~1.5 deg.s^{-2}, and increase monotonically for frequencies above 0.5 Hz. This suggests that there could be an acceleration threshold (79.4% correct detection criterion) for frequencies below 0.5 Hz, just as there is a velocity threshold for frequencies above 0.5 Hz. In other words, for frequencies below 0.5 Hz of the input stimulus, motion will be correctly detected 79.4% of the time if the peak acceleration attained is $\geq a_{thresh}$ = 1.5 deg.s^{-2}. Grabherr et. al. proposed a high pass filter model for thresholds, as a result of which the threshold was a velocity threshold at high frequencies and an acceleration threshold at low frequencies.

Now, the question is, is the threshold for motion perception, an acceleration threshold below 0.5 Hz and a velocity threshold for frequencies ≥ 0.5 Hz? Arguably not. These two thresholds could well exist together for all frequencies, and for motion perception, both thresholds have to be crossed. The details of the single cycle sinusoidal acceleration stimuli used by Grabherr et. al. are shown below:

$$a = A\sin(2\pi ft) \text{ - Acceleration profile of the stimulus}$$

$$v = \frac{A}{2\pi f}(1-\cos(2\pi ft)) \text{ - Corresponding cosine bell velocity profile}$$

$$a_{peak} = A \text{ deg.s}^{-2} \qquad (4.1)$$

$$v_{peak} = \frac{A}{\pi f} \text{ deg.s}^{-1} \qquad (4.2)$$

where A is the amplitude, and f is the frequency of the acceleration stimulus. a_{peak} is the peak acceleration attained and v_{peak} is the peak velocity attained by the stimulus.

It can be seen from Table 5.1 that for frequencies above 0.5 Hz, $a_{peak} > a_{thresh}$. For these frequencies, a sinusoidal stimulus of amplitude a_{thresh} would not meet the velocity threshold because $v_{peak} = \frac{a_{peak}}{\pi f} < v_{thresh}$. Hence, for motion to be detected, a_{peak} should be sufficiently larger than a_{thresh}.

Similarly, for frequencies below 0.5 Hz, $v_{peak} > v_{thresh}$. For these frequencies, stimuli with $v_{peak} = v_{thresh}$ would not meet the acceleration threshold because $a_{peak} = v_{peak}(\pi f) < a_{thresh}$. Therefore, to detect motion, v_{peak} should be sufficiently larger than v_{thresh}, which explains the increasing threshold with decreasing frequency.

5.1 HYPOTHESIS

For motion perception of sinusoidal acceleration stimuli, there exist two-thresholds - a constant velocity threshold v_{thresh} and a constant acceleration threshold a_{thresh} for all frequencies, and the subject would detect motion (79.4% correct criterion) only if the peak velocity and the peak acceleration attained by the stimuli are above their respective threshold values. This is a somewhat different scheme than hypothesized in the literature. For example, Grabherr, et al (2008) proposed model where the angular velocity estimate was high pass filtered, and fed to a single threshold. The effect of the high pass filter was to make the single threshold element act as a velocity threshold for higher frequencies and acceleration threshold for lower frequencies. However, the hypothesis for the model in this chapter assumes that the CNS computes both a velocity and acceleration estimate, and both determine the threshold behavior.

5.2 TWO-THRESHOLD MODEL

Based on the two-threshold hypothesis, a model for motion detection is proposed in the following paragraphs.

From equation (5.2), it can be seen that the peak acceleration and peak velocity attained are determined by amplitude and frequency of the sinusoidal stimulus. It is to be noted that v_{peak} and a_{peak} occur at different instants - v_{peak} occurs at $T/2$ and a_{peak} occurs at $T/4$, where $T = \frac{1}{f}$ is the time period . Yet, according to the hypothesis, it is their combination that decides if the stimulus will be detected or not. There are two possible explanations for this:

The first possibility is the effect of memory. When the subject is experiencing v_{peak} , he remembers that he had experienced a_{peak} sometime back, and correlates the two. But this hypothesis has its weaknesses. During a test, when a subject is paying attention to the stimulus, he may have a harder time recalling a property of the stimulus (a_{peak} or v_{peak}) that occurred several seconds earlier back; he will be concentrating more on the present sensation. This possibility also does not also take into account the perception of motion

that the subject would get by observing the other instances of the stimulus. In other words, this hypothesis suggests that all what a subject cares about is just two specific instances during the stimulus (a_{peak} and v_{peak}) and makes his decision based on that, which is not quite convincing.

The second and more plausible explanation is the following:

Although presented with a continuous stimulus, the subject could be sampling the CNS angular velocity estimates and detecting motion on each of those sampling instances. If the subject had perceived motion on a sufficient number of these sampling instances, he is willing to decide that he has moved. This sampling process could be very similar to the sampling that occurs in vision, which causes the wagon-wheel effect (stroboscopic) effect. This vestibular sampling frequency could be fairly high to capture the instantaneous rate of change of the CNS angular velocity estimate (i.e perceived acceleration) to a reasonable degree of accuracy.

Let us consider a case where the perceived noise-free acceleration and velocity profiles look like what are shown in Fig. 5.1 and Fig. 5.2 respectively. (These are just notional sketches and are not real simulations). With noise, they would look as shown in Fig. 5.3 & Fig. 5.4. The noise is in the perceived velocity and the perceived acceleration is the derivative of perceived velocity.

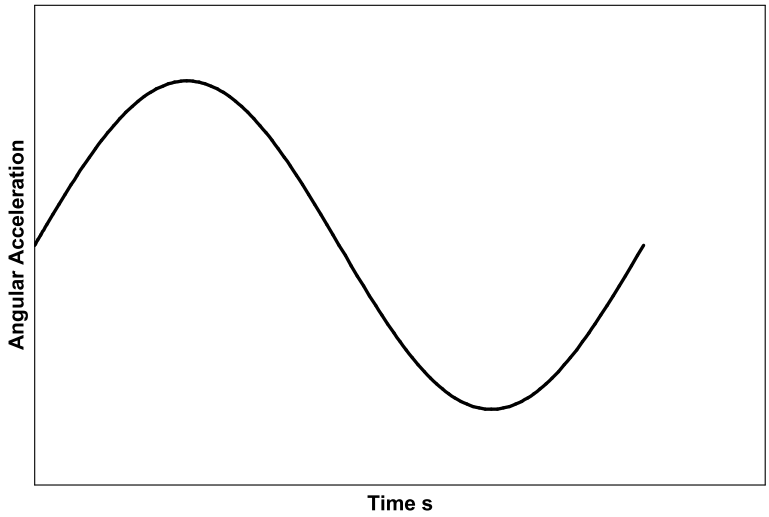

Fig. 5.1 – Perceived angular acceleration without noise

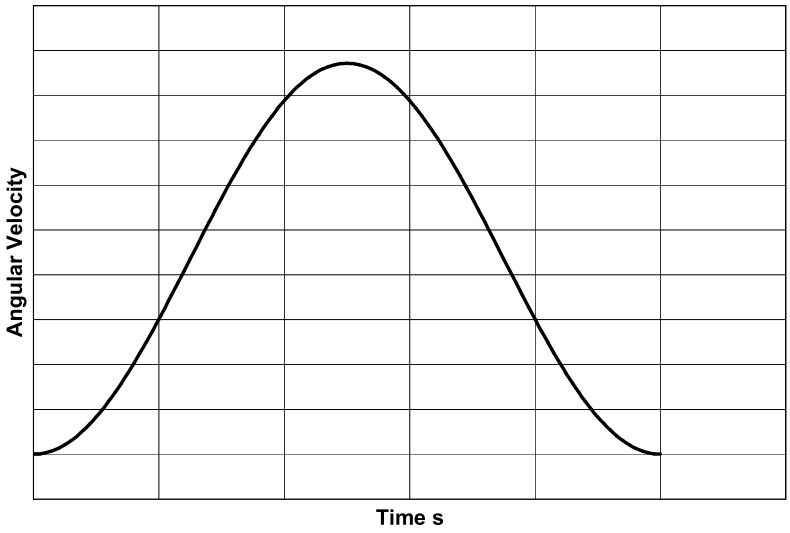

Fig. 5.2 – Perceived angular velocity without noise

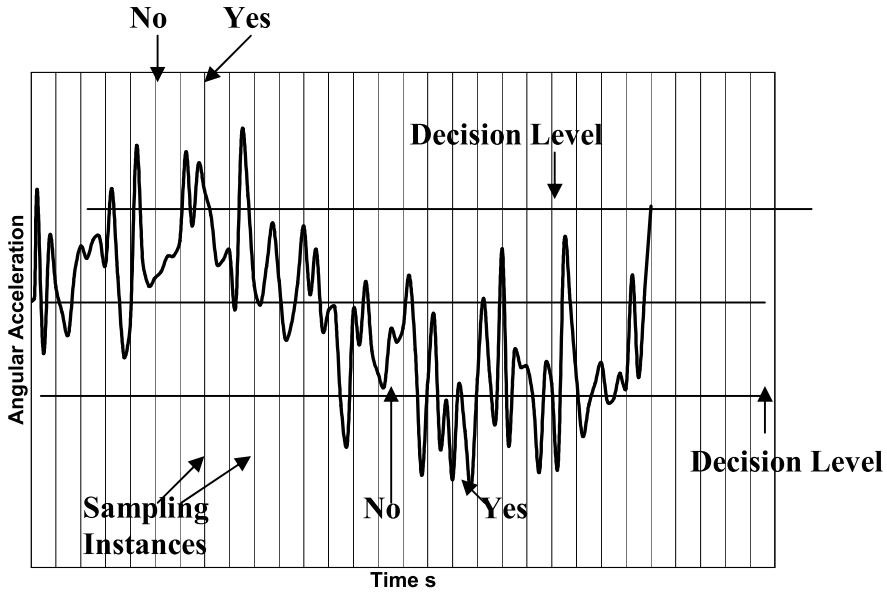

Fig. 5.3 – Perceived angular acceleration corrupted by noise

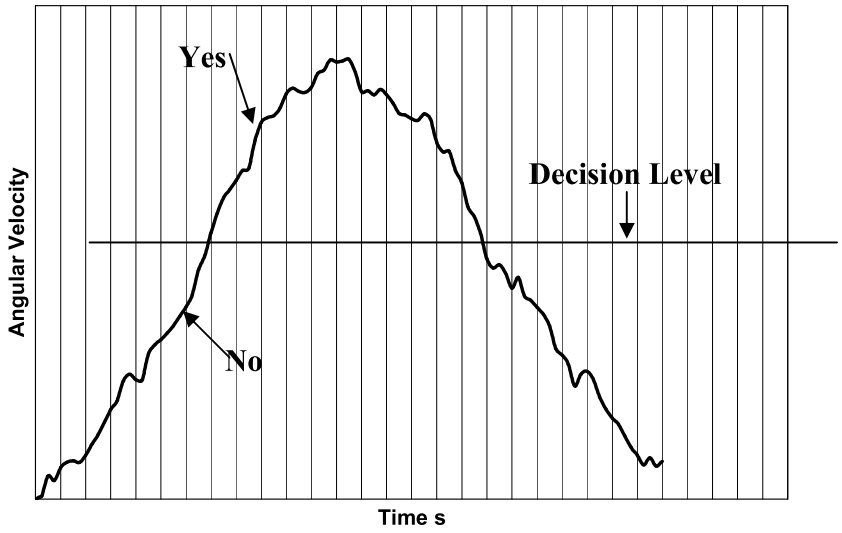

Fig. 5.4 – Perceived angular velocity corrupted by noise

The vertical lines in Fig. 5.3 & Fig. 5.4 show the instances at which the perceived noisy acceleration and perceived noisy velocity are sampled. A decision level is the threshold level which the instantaneous acceleration and velocity have to cross for the subject to decide that he is moving at that time instant (a 'Yes' response). Note the decision levels for acceleration and velocity are not equal to a_{thresh} and v_{thresh}, but less than them respectively. This is because a_{thresh} and v_{thresh} are thresholds on the global **peak** acceleration and velocity and not on the **instantaneous** acceleration and velocity. To highlight this difference, the term 'decision level' is used for the instantaneous acceleration and velocity. Fig. 5.3 shows that in the noise-free case, the instantaneous acceleration and velocity would be consistently outside (i.e. above the decision level if positive and below the level if negative) the decision level in an interval. However, if noise is present, they could be brought within the decision level, as shown in Fig. 5.4. This would make the subject decide that he is not moving ('No'). Therefore, the hypothesis says that when subjected to a stimulus, the subject keeps evaluating if he is moving ('Yes') or not ('No') at various instants. This is very similar to how a subject would respond in reality when rotated.

An interesting case comes when only one of acceleration or velocity crosses the decision level, whereas the other does not. In such a case, it is hypothesized that to perceive motion ('Yes'), both velocity and acceleration have to be outside the decision level. So when a stimulus is presented, the subject samples it at various points and chooses a 'Yes' response at an instant if the instantaneous acceleration and velocity are outside his personal decision level. After the stimulus is presently completely, if there are a good number of 'Yes' responses, the subject finally decides that he has moved.

The two-threshold model for yaw perception can be schematically represented as shown in Fig. 5.5

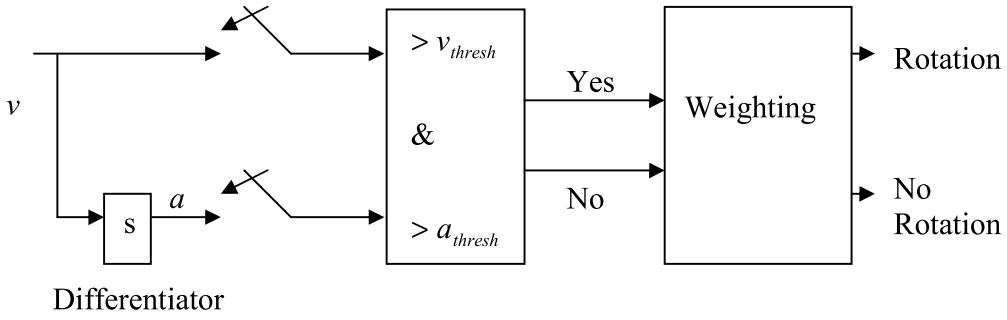

Fig. 5.5 – Two-Threshold model for Yaw Perception

The two-threshold model was designed using threshold values from Grabherr's data. The decision levels for v and a were chosen to be half v_{thresh} and a_{thresh} respectively. Therefore, if the instantaneous velocity is above $v_{thresh}/2 = 0.71$ deg.s^{-1} and the instantaneous acceleration is above $a_{thresh}/2 = 0.75$ deg.s^{-1}, the subject would decide that he is moving at that time instant. The noise in the perceived velocity was assumed to be Gaussian and white. The variance of the noise was chosen such that the spurious acceleration sensation it would cause when the velocity is a constant, is well below the acceleration decision level. Going by this argument, and assuming a 3σ limit, we have

$$3\frac{\sigma_{velocity}}{\Delta t} = 0.75 \text{ deg.s}^{-2}$$

where Δt is the time interval between successive samples. If the sampling frequency is constant, then $\Delta t = \frac{1}{f_{samp}}$. For this simulation was assumed that the sampling frequency is 200 Hz, because VOR evoked by electrical stimulation could be as high as 150 Hz, and hence, vestibular sampling frequency could be higher than this value. (The sampling frequency is hypothetical of course; there has been no prior research in sampling in vestibular perceptions).

$$\Delta t = \frac{1}{f_{samp}} = \frac{1}{200} = 0.005$$

$$\Rightarrow \sigma_{velocity} = 0.00125 \text{ deg.s}^{-1}$$

As can be seen from the calculation above, the sampling frequency is a critical parameter for the model and determines the variance of the Gaussian noise assumed. The acceleration at any time instant *n* can be computed by a finite difference method as,

$$a_n = \frac{v_{n+1} - v_n}{\Delta t}$$

The subject would decide he is moving at any given instant if

$$v_n \geq 0.71\,\text{deg.s}^{-1}$$

and

$$a_n \geq 0.75\,\text{deg.s}^{-1}$$

The direction of motion as perceived by the subject is given by the direction of the instantaneous acceleration.

Once the entire stimulus is presented, presumably the subject has to have a reasonable number of 'Yes' responses to believe that he has moved. This 'reasonable number' is termed a confidence metric. This ideally should be 50%, but it could be any value near to 50%. This strongly relates to the issue of 'decision bias' – how certain the subject wants to be. This value also depends on the subject's memory, as to how many 'Yes' or 'No' responses he forgets. However, for the model constructed, the percentage of 'yes' responses is computed for the entire duration of the stimulus and if this number is greater than the confidence metric, the subject finally decides that he has experienced rotation.

For testing the model, the perceived noisy velocity input to the detector was obtained by sampling the output from *Observer* for the single cycle sinusoidal acceleration stimulus, and adding Gaussian noise of $\sigma_{velocity} = 0.00125$ deg.s^{-1}. The perceived noisy velocity was then fed into the two-threshold detector. The results are presented in detail in Chapter 6.

CHAPTER 6: RESULTS AND DISCUSSION

6.1 MATCHED FILTER THRESHOLD MODEL

As stated in chapter 4, detection threshold values (assuming decision bias resulting in 79.4% correct detection) derived from Grabherr's study were used to check model detection performance.

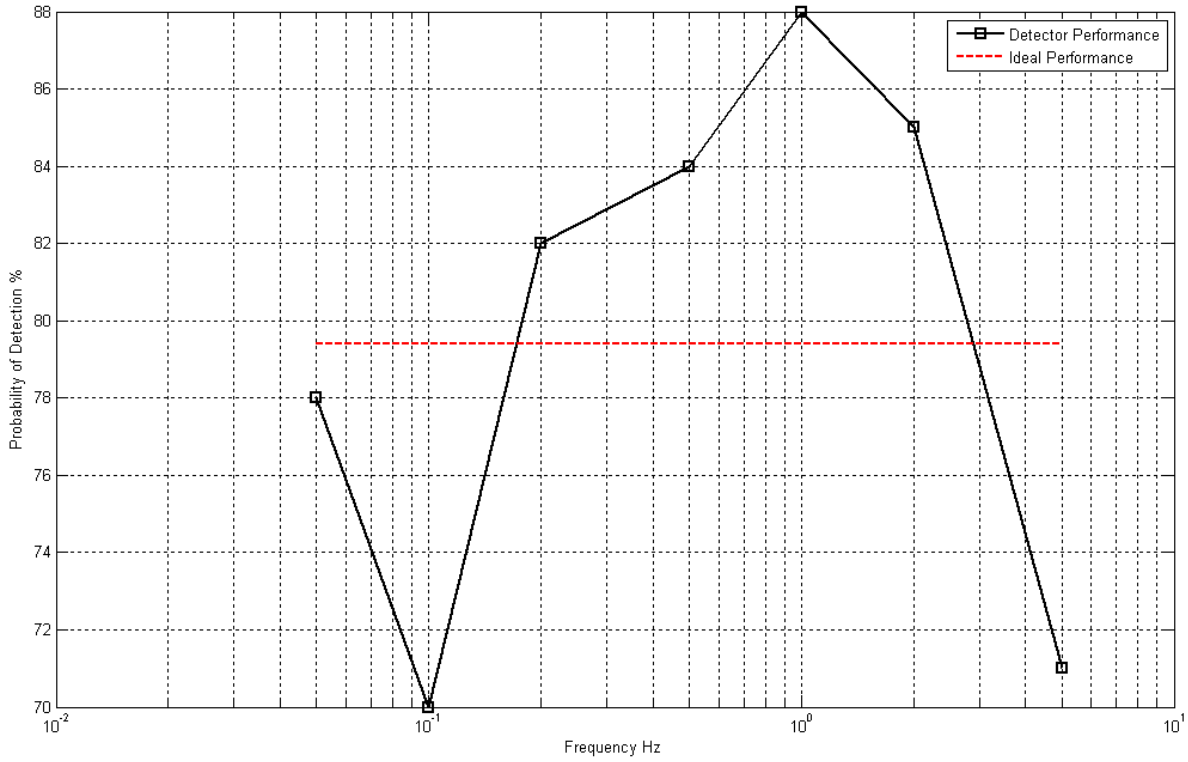

Fig. 6.1 – Performance of the Matched Filter Model for Thresholds

Monte Carlo simulations were done with sinusoidal acceleration stimuli of detection threshold amplitude A_{det} input to *Observer* for many trials and the resulting perceived yaw velocity output corrupted with Gaussian noise of σ = 1.42 deg.s^{-1} tested with the matched filter detector. The percentage of time the detector correctly detects the stimulus is a measure of its performance. Since detection thresholds for 79.4% correct detection criterion were used, if the detector's performance is also close to 79.4%, it means that the detector is good.

The performance of the detector is shown in Fig. 6.1. As can be seen, the matched-filter detector generally produces good performance and is able to match Grabherr's data reasonably with an error of 10%

As mentioned earlier drawback with this model is that it applies only to the Grabherr paradigm where the subject knows the stimulus waveform. It is not clear how to choose the threshold for $T(\mathbf{x})$ for unknown - stimuli. It assumes the subject's decision bias $\sqrt{\gamma'}$ is known. Also, the detector does not respond till the stimulus is complete – it does not describe the instantaneous perception of motion and only tells if there was a motion stimulus or not after it is completely administered. Hence it cannot capture instantaneous perceptual phenomena and hence is not so useful for modeling spatial disorientation illusions.

6.2 TWO THRESHOLD MODEL

Detection threshold values (again assuming a decision bias appropriate for 79.4% correct detection) derived from Grabherr's study were used to evaluate the model.

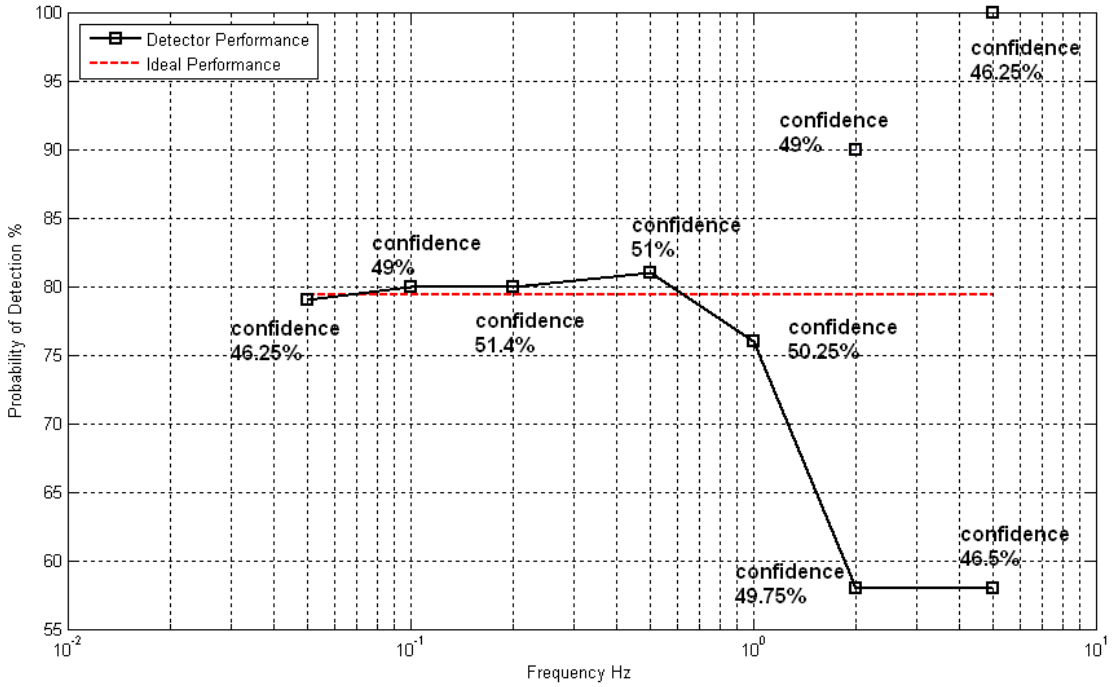

Fig. 6.2 – Performance of the two-threshold detector model

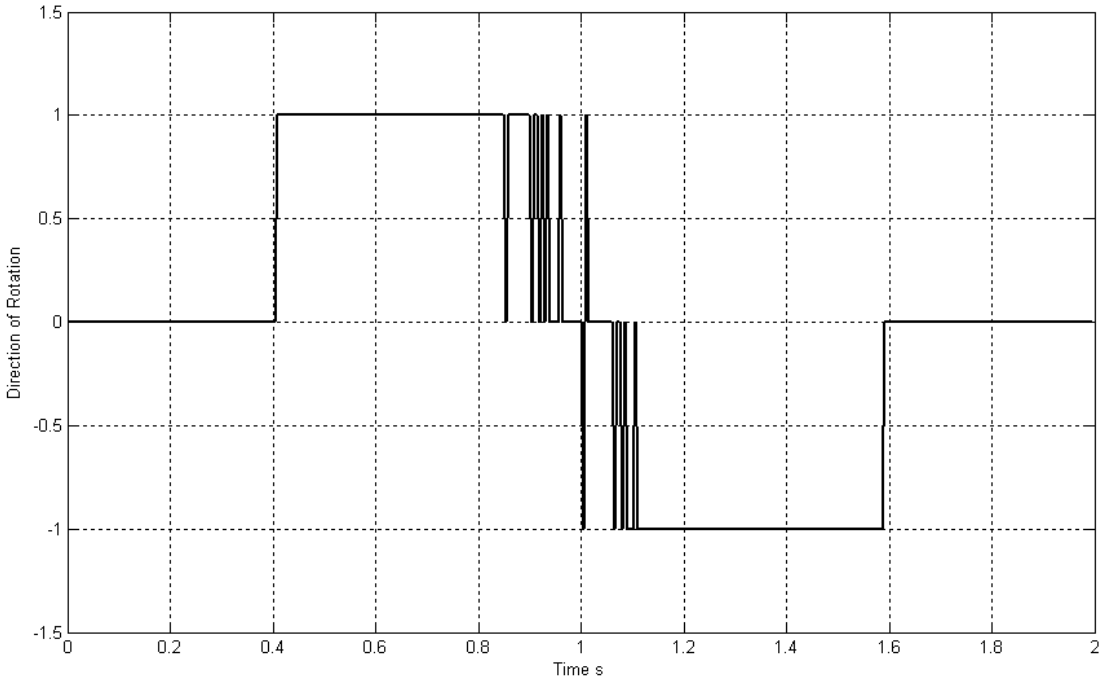

Fig. 6.3 - Instantaneous Perception of Direction of Movement During the Course of a Threshold Stimulus

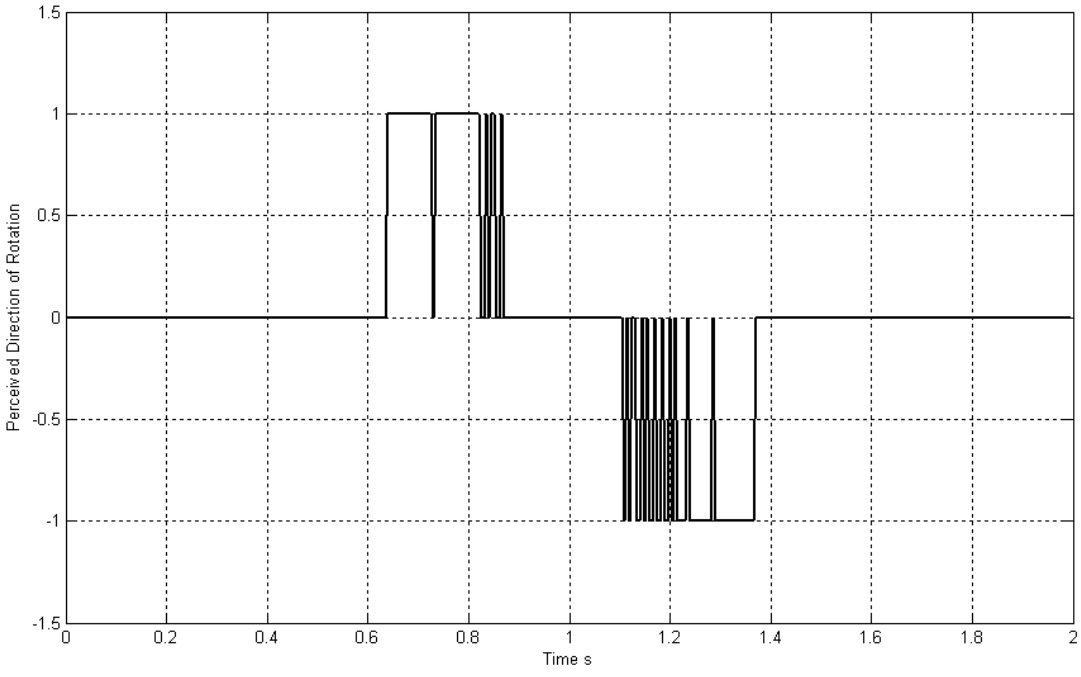

Fig. 6.4 – Instantaneous Perception of Motion During the Course of a Sub-Threshold Stimulus

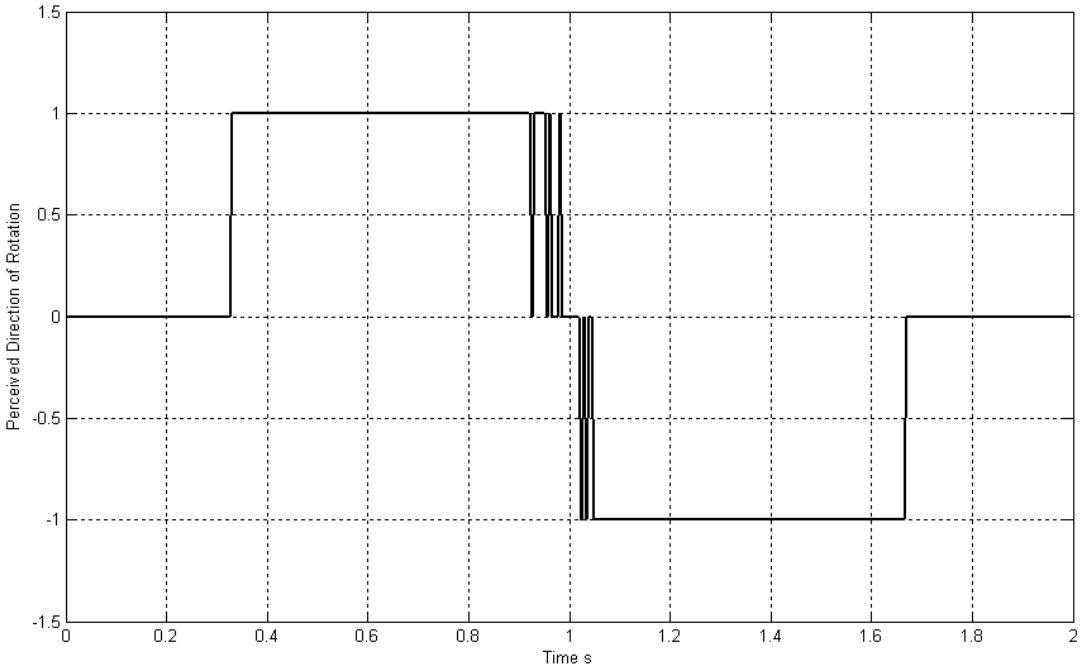

Stimulus

To check the model, a single cycle sinusoidal acceleration stimulus of detection threshold amplitude A_{det} was input to *Observer* and the resulting perceived yaw velocity from the output was corrupted with Gaussian noise of $\sigma = 0.00125$ deg.s^{-1}. In the detector, the perceived noisy velocity was differentiated using a finite difference method to obtain the noisy acceleration. The instantaneous noisy velocity and acceleration were compared with their decision levels (half the threshold values were chosen for the model) and the perception of rotation at each instant of time is evaluated. Once the stimulus is completely presented, the percentage of 'Yes' responses was counted and if this value was above a confidence metric, the detector says an overall 'Yes' for the existence of the stimulus. Monte Carlo simulations were carried out repeating this process for many trials and the percentage of time the detector correctly detects the stimulus is a measure of its performance. Since detection thresholds for 79.4% correct detection criterion were used, if the detector's performance is also close to 79.4%, it means that the detector matches the data.

Detection threshold stimuli at the 7 frequencies used in Grabherr's study were used for validation and the performance of the detector is shown in Fig. 6.2. In each case, it was found that the two-threshold detector was able to meet the 79.4% correct detection criterion by proper tuning of the confidence metric. The confidence metric in each case for 79.4% correct detection is shown in Fig. 6.2. The difference in confidence metrics in

each case can be explained by the fact that the subject would be only vaguely setting this value (decision bias, as explained earlier), and is hence prone to certain error. Also, it was assumed that the confidence metric remains the same in all runs of the simulation, at a particular frequency. However, when a subject is tested repeatedly, he might change this value from one trial to another. As explained in chapter 5, this value is also affected by the memory of the subject.

It can be seen from the Fig. 6.2 that for frequencies 2 Hz and 5 Hz, a very small change in confidence metric causes great change in performance. This high sensitivity shows that the stimuli are of threshold level, and they could be easily missed if the subject even slightly makes an error in remembering the number of 'Yes' responses he has made. It can also be inferred from Fig. 6.2 that there must be confidence metric between the two values shown for 2 Hz and 5 Hz that gives 79.4% correct detection performance.

Fig. 6.3 shows the plot of the subject's instantaneous perception of direction of rotation during the course of a threshold stimulus to the right. A value of +1 corresponds to rotation to the right and -1 corresponds to rotation to the left. A value of 0 corresponds to no rotation. It can be seen that the number of instances during which perception of motion exists is roughly equal to the number of instances during which there is no perception of motion. It can also be seen that until a certain time after the stimulus begins, no motion is perceived by the subject as both the instantaneous velocity and acceleration are within their decision levels. Thereafter, he perceives motion towards right. However, even while experiencing rotation, the subject gets doubts about not moving every now and then, due to noise. After a while, the perceived direction of rotation completely reverses. This explains why subjects tend to feel rotation in the opposite direction although presented with rotation in only one direction, as reported by Benson et. al. (1989). The two-threshold model is therefore able to explain experimental phenomena and also able to meet the 79.4% correct detection performance at various frequencies.

Fig. 6.4 shows the perceived instantaneous direction of rotation for a sub-threshold stimulus to the right. It can be seen that the number of instances during which rotation is perceived is significantly lesser than the number of instances during which no rotation is perceived, and lesser than that of the threshold stimulus.

Fig. 6.5 shows the perceived instantaneous direction of rotation for a supra-threshold stimulus to the right. It can be seen that the number of instances during which rotation is perceived is significantly higher than the number of instances during which no motion is perceived, and higher than that of the threshold stimulus.

Thus the prediction of the two-threshold model agrees with what is expected for these kinds of stimuli.

The two-threshold model can also be evaluated using the following thought experiment:

Let us imagine that a subject is yawed at sub-threshold level in one direction and then reversed direction and yawed at supra-threshold level and then brought to rest, as shown in Fig. 6.6.

-

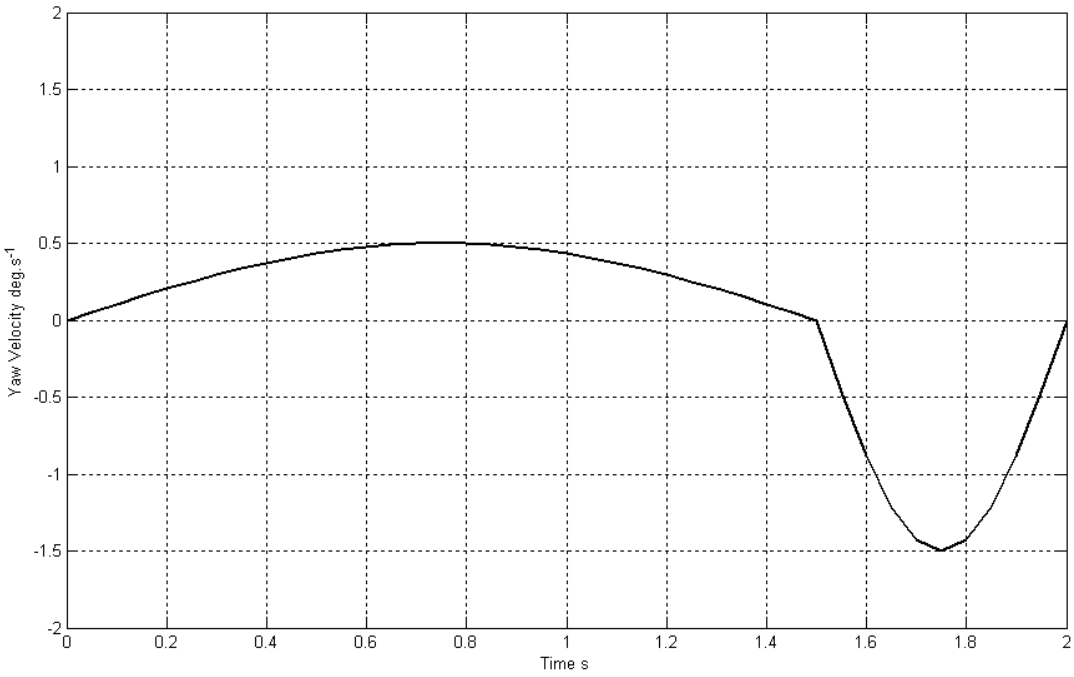

Fig. 6.6 Plot of a motion profile with sub-threshold yaw to the right followed by supra-threshold yaw to the left

The time in Fig. 6.6 is only representative. Suppose, the area under the first half cycle is equal and negative to the area under the second half cycle, the net displacement in azimuth would be zero. The azimuth prediction from *Observer* without thresholds be close to zero, as it will predict that rotation first occurred to the right and then reversed.

However, because the stimulus in the first half-cycle was below threshold, this rotation would not be perceived and only the supra-threshold yaw in the second half-cycle will be perceived. This behavior is predicted by the two-threshold model as shown in Fig. 6.7. Therefore, once the experiment is over, the subject would have a large error in the estimation of azimuth. The model correctly predicts that there would be no perception of rotation up till some instant in the second half-cycle. Thereafter, the subject would feel that he had **started** rotating in the opposite direction to the original direction of rotation.

The perceived direction of rotation then reverses and towards the end, there is no perception of motion.

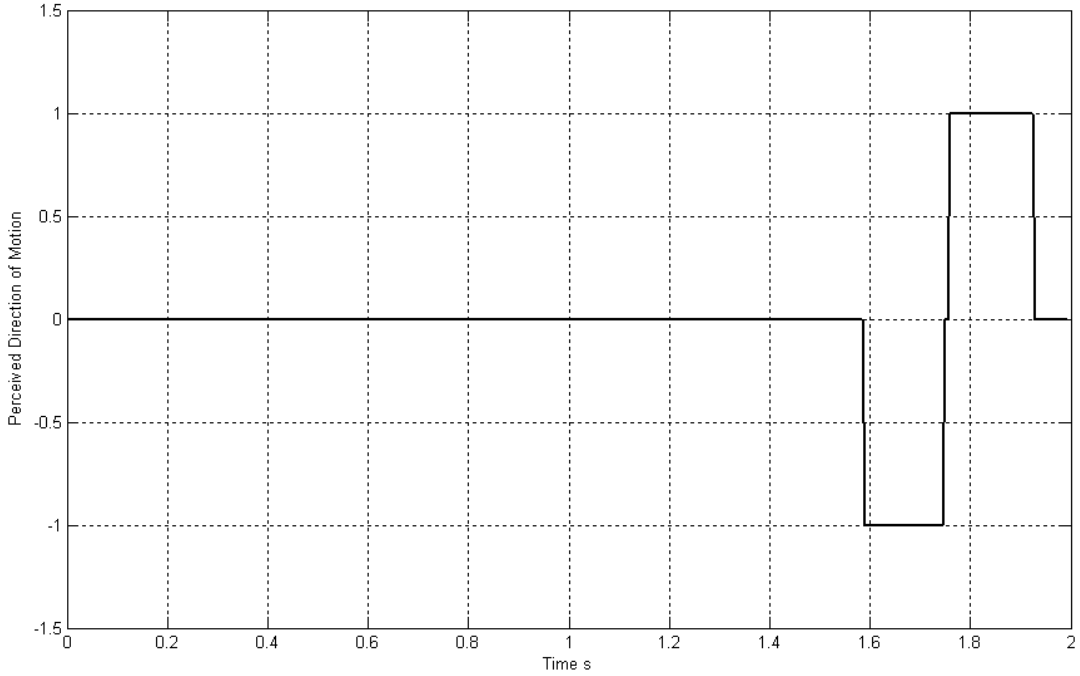

Fig. 6.7 Perceived direction of motion as predicted by the two-threshold model for the example

If the above example happens in the case of roll motion, it results in “the leans” illusion. The example was explained in yaw because a similar model for roll is not yet developed, mainly because comprehensive data on roll thresholds like that of yaw are not available.

The two-threshold model is therefore able to mimic the instantaneous perception of motion during the course of a stimulus and also account for spatial disorientation illusions

CHAPTER 7: CONCLUSIONS AND REMARKS

The matched filter detector model for thresholds discussed in Chapter 4 shows that it can produce good performance, but is applicable only to sinusoidal stimuli. This prevents it from being used for other types of stimulus profiles.

Also, this model is not capable of predicting instantaneous perception of rotation and hence not good for predicting illusions. This model can only say if the stimulus was present or not **after** the stimulus is over and cannot say anything about how the perception of motion changes with time when subjected to motion. Also theoretically sound, it is not so convincing that the Central Nervous System estimator might be evaluating thresholds through such a template correlation like scheme in the matched-filter model. Although it matches Grabherr's data it doesn't seem to be a plausible model of the decision process..

The two-threshold model for thresholds developed has the ability to predict instantaneous perception of rotation and spatial disorientation illusions because it operates on instantaneous samples. The model uses simple logic to decide on the perception of motion, unlike the matched filter detector which uses a complicated correlation. This simple logic is how a normal human could use to detect motion, so there are more convincing reasons to believe that the two-threshold model could be a good model of the CNS detection process.

To test the two-threshold model hypothesis, the following experiment is proposed:

For checking the acceleration threshold, administer a velocity ramp stimulus (an acceleration step) to the subject, making sure that the magnitude of acceleration is around the decision level for acceleration ($a_{thresh}/2$), and check if the stimulus is detected at all. If the stimulus is never detected, it would prove the hypothesis and the value of acceleration used for the trial is the decision level for acceleration. If the stimulus is detected, reduce the acceleration and repeat the stimulus again till it is not recognized. If no minimum limit is found on the acceleration value, it would disprove the hypothesis.

For checking the velocity threshold, administer a velocity ramp with acceleration greater than the acceleration decision level, and ask the subject to report **when** he starts perceiving motion and record this time. This recorded time would also have reaction time in it. However, if the reaction time is carefully subtracted from the data, the remainder is latency time. Then derive the product (acceleration value) X (latency time). (This is equivalent to the Mulder's law). If this product is a constant, it would prove one part of

the hypothesis. If the product is not a constant, the two-threshold hypothesis would be disproved.

Strong motion cues to the subject could occur if the stimuli are begun and ended abruptly during the experiments. So care must be to taken to smooth the test stimulus profile at its ends and so, steps in accelerations should be avoided. This will make the test stimulus different from a velocity ramp at the beginning and at the end.

Both these models assume detection threshold values which are twice the recognition threshold values reported in the literature. This is another major assumption but could be experimentally investigated. It is probably be valid for all subjects. If the subject's penalty for a false alarm is increased, the probability of false alarms would change and so would the detection threshold in such a case.

The lack of availability of data for other motions perceptions simillar that of yaw makes modeling other thresholds of motion difficult. Therefore, to model other motion perception thresholds, more data is needed, preferably their variation as a function of frequency. Also, a trend like in yaw motion may not exist for other thresholds. In such cases, appropriate experiments have to be done to reveal any likely trends.

To fully develop *Observer* for use in accident investigation and flight simulator design, a whole set of thresholds on angular and linear motion, and vision have to be incorporated. However, incorporating these thresholds is hampered by the unavailability of enough experimental data. So future research should focus on devising experiments that would help in modeling thresholds better.

REFERENCES

Benson, A. J., Spencer, M. B., and Stott, J. R. R., 1986, “Thresholds for the Detection of the Direction of Whole-Body, Linear Movement in the Horizontal Plane,” Aviation Space and Environmental Medicine, Vol. 57, pp. 1088-1096.

Benson, A. J., Hutt, E. C. B., and Brown, S. F., 1989, “Threshold for the Perception of Whole-Body Angular movement About a Vertical Axis”, Aviation Space and Environmental Medicine, Vol. 60, pp. 205-213.

Borah, J., Young, L. R., Curry, R. E., 1988, “Optimal Estimator Model for Human Spatial Orientation”, Annals New York Academy of Sciences.

Bringoux, L., Schmerber, S., Nougier, V., Dumas, G., Barraud, P. A., Raphel, C., 2002, “Perception of Slow Pitch and Roll Body Tilts in Bilateral Labyrinthine-Defective Subjects”, Neuropsychologia 40(2002) 367-372.

Clark, B., Stewart, J., 1962, "Perception of Angular Acceleration About the Yaw Axis of a Flight Simulator - Thresholds and Reaction Latency for Research Pilots", Aerospace Medicine.

Clark, B., 1967, “Thresholds for the Perception of Angular Acceleration in Man”, Aerospace Medicine, Vol. 38, No. 5.

Clark, B., Stewart, J., 1969, "Effects of Angular Acceleration on Man: Thresholds for the Perception of Rotation and the Oculogyral Illusion", Aerospace Medicine.

Cornsweet, T. N., 1962, “The Staircase-Method in Psychophysics”, The American Journal of Psychology, Vol. 75, No. 3, pp. 485-491.

Fernandez, C., Goldberg, J. M., 1976, “Physiology of Peripheral Neurons Innervating Otolith Organs of the Squirrel Monkey. I. Response to Static Tilts and to Long Duration Centrifugal Force”, Journal of Neurophysiology, Vol. 39, No. 5.

Goldberg, J. M., Fernandez, C., 1971, “Physiology of Peripheral Neurons Innervating Semicircular Canals of the Squirrel Monkey. I. Resting Discharge and Response to Constant Angular Accelerations”, Journal of Neurophysiology, 34:635-660.

Grabherr, L., Nicoucar, K., Mast, F. W., Merfeld, D. M., 2008, “Vestibular Thresholds for Yaw Rotation About an Earth-Vertical Axis as a Function of Frequency”, Exp Brain Res (2008) 186:677-681, Springer-Verlag.

Groen, J. J., Jongkees, L. B. W., 1948, “The threshold of angular acceleration perception”, Journal of Physiology.

Guedry, F. E., 1974, “Psychophysics of Vestibular Sensation Chapter 1, Handbook of Sensory Physiology”, Vol. 6, edited by H. H. Kornhuber, Springer-Verlag, Berlin, pp. 3-154.

Gundry, A. J., 1978, "Experiments on the Detection of Roll Motion", Aviation, Space, and Environmental Medicine.

Gundry, A. J., 1978, “Thresholds of Perception for Periodic Linear Motion”, Aviaton, Space and Environmental Medicine.

Jones, G. M., Young, L. R., 1976, "Subjective detection of vertical acceleration: A velocity dependent response?", DRB Aviat. Med. Res. Unit Rep. 5:245-255; Report No. DR 225.

Kay, S. M., 1998, “Fundamentals of Statistical Signal Processing, Volume 2: Detection Theory”, Prentice Hall, 1st Edition.

Leek, M. R., 2001, “Adaptive Procedures in Psychophysical Research”, Perception & Psychophysics, 63(8), 1279-1292.

Mah, R. W., Young, L. R., Steele, C. R., Schubert, E. D., 1989, “Threshold Perception of Whole-Body Motion to Linear Sinusoidal Stimulation”, AIAA Flight Simulation Technologies Conference and Exhibit, AIAA-89-3273.

Meiry, J. L., 1965, “The Vestibular System and Human Dynamic Space Orientation”, Thesis, Massachusetts Institute of Technology.

Merfeld, D. M., 2010, “Paradigm Comparisons”, Manuscript, personal communication.

Mulder, W., 1908, “Quantitatieve betrekking tusschen prikkel en effect bij het statisch organ”, Thesis, Rijks University of Utrecht.

Newman, M., 2009, “A Multisensory Observer Model for Human Spatial Orientation Perception”, Thesis, Man Vehicle Laboratory, MIT.

Ormsby, C. C., Young L. R., 1977, “Integration of Semicircular Canal and Otolith Information for Multisensory Orientation Stimuli”, Mathematical Biosciences 34, 1-21 (1977).

Sivan, R., Ish-Shalom, J., Huang, J. K., 1982, “An Optimal Control Approach to the Design of Moving Flight Simulators”, IEEE Transactions on Systems, Man, and Cybernetics, Vol. SMC-12, No. 6.

Snow, J., Wackym, P., Ballenger, J., 2009, *Ballenger's Otorhinolaryngology: Head and Neck Surgry.* Shelton, Conn: People's Medical Pub. House/BC Decker.